New Rotation Periods in the Open Cluster NGC 1039 (M 34), and a Derivation of its Gyrochronology Age.

David J. James[1,2], Sydney A. Barnes[3], Søren Meibom[4], G. Wesley Lockwood[3], Stephen E. Levine[5], Constantine Deliyannis[6], Imants Platais[7], Aaron Steinhauer[8], and Briana K. Hurley[1]

[1] Hōkū Ke'a Observatory, Department of Physics & Astronomy, University of Hawai'i at Hilo, 200 West Kawili Street, Hilo, HI 96720, USA: e-mail: david.james@hawaii.edu
[2] Department of Physics & Astronomy, Vanderbilt University, Box 1807 Station B, Nashville, TN 37235, USA
[3] Lowell Observatory, 1400 W. Mars Hill Rd., Flagstaff, AZ 86001, USA
[4] Harvard-Smithsonian Center for Astrophysics, 60 Garden Street, Cambridge, MA 02138, USA
[5] United States Naval Observatory, Flagstaff Station, 10391 West Naval Observatory Road, Flagstaff, AZ 86001-8521, USA
[6] Astronomy Department, Indiana University, Swain Hall West 319, 727 East 3rd Street, Bloomington, IN 47405-7105, USA
[7] Department of Physics & Astronomy, Johns-Hopkins University, Baltimore, MD 21218, USA
[8] Department of Physics and Astronomy, 1 College Circle, SUNY Geneseo, Geneseo, NY 14454, USA

ABSTRACT

Aims. Employing photometric rotation periods for solar-type stars in NGC 1039 [M 34], a young, nearby open cluster, we use its mass-dependent rotation period distribution to derive the cluster's age in a distance independent way, i.e., the so-called gyrochronology method.

Methods. We present an analysis of 55 new rotation periods, using light curves derived from differential photometry, for solar type stars in the open cluster NGC 1039 [M 34]. We also exploit the results of a recently-completed, standardized, homogeneous BVIc CCD survey of the cluster, performed by the Indiana Group of the WIYN open cluster survey, in order to establish photometric cluster membership and assign B-V colours to each photometric variable.

We describe a methodology for establishing the gyrochronology age for an ensemble of solar-type stars. Empirical relations between rotation period, photometric colour and stellar age (gyrochronology) are used to determine the age of M 34. Based on its position in a colour-period diagram, each M 34 member is designated as being either a solid-body rotator (*interface or I-star*), a differentially rotating star (*convective or C-star*) or an object which is in some transitory state in between the two (*gap or g-star*). Fitting the period and photometric colour of each I-sequence star in the cluster, we derive the cluster's mean gyrochronology age.

Results. Of the photometric variable stars in the cluster field, for which we derive a period, 47 out of 55 of them lie along the loci of the cluster main sequence in V/B-V and V/V-I space. We are further able to confirm kinematic membership of the cluster for half of the periodic variables [21/55], employing results from an on-going radial velocity survey of the cluster. For each cluster member identified as an I-sequence object in the colour-period diagram, we derive its individual gyrochronology age, where the mean gyro age of M 34 is found to be 193 ± 9 Myr.

Conclusions. Using differential photometry, members of a young open cluster can be easily identified in a colour-magnitude diagram from their periodic photometric variability alone. Such periodicity can be used to establish a period-colour distribution for the cluster, which for M 34, we have used to derive its gyrochronology age of 193 ± 9 Myr. Formally, our gyro age of M 34 is consistent (within the errors) with that derived using several *distance-dependent*, photometric isochrone methods (250 ± 67 Myr).

Key words. Methods: data analysis – Stars: starspots – Galaxy: open clusters and associations: NGC 1039 – Stars: fundamental properties (age)

1. Introduction

Over the past century, as instrumentation and detector technology have advanced, the methods by which stellar age is determined have also evolved. While we still rely heavily upon the use of theoretical model isochrones, fitting empirical luminosity-temperature data (on an H-R diagram - e.g., Sandage 1958; Demarque & Larson 1964; Demarque & Gisler 1975, Mengel et al. 1979; and more latterly, Meynet, Mermilliod & Maeder 1993; D'Antona & Mazzitelli 1997; Naylor 2009), several alternative techniques for determining stellar age now exist which exploit a more diverse assembly of fundamental stellar properties, such as magnetic activity, elemental abundances, white dwarf cooling time-scales and angular momentum content.

Inspired by the pioneering efforts of Wilson (1963), observations of solar type stars have shown that there is a clear age dependence in the strength of magnetic activity indicators (eg., Ca II H & K and X-rays), whose emissions are presumably due to solar-like magnetic field activity (eg., Wilson 1964; Wilson & Skumanich 1964; Wilson 1966; Skumanich 1972; Barry et al. 1981; Noyes et al. 1984; Maggio et al. 1987; Soderblom, Duncan & Johnson 1991; Henry et al. 1996; Mamajek & Hillenbrand 2008). While there is not a one-to-one relationship between activity and age for any given star, current data samples unequivocally show there to be a strong correlation between decreasing magnetic activity and increasing age.

However, even such a well-observed phenomenon does not deliver unequivocal results, as illustrated for instance by the factor of two range in ages derived by Giampapa et al. (2006) for

photometric and kinematic members of the 4Gyr-old open cluster M 67. Moreover, stellar activity cycles, akin to those occurring in the Sun, can also lead to difficulties in establishing ages for individual stars. For instance, Soderblom et al. (1991) show that errors on chromospheric ages are roughly 50%. Presumably, this error could be driven down statistically in a cluster by measuring many stars, and by removing close binaries or other contaminants. Soderblom, Jones & Fischer (2001) have provided chromospheric Hα measurements for a significant number of M 34 stars, but to our knowledge, a chromospheric age for M 34 has not yet been published.

More recently, age determinations for young open clusters have been advanced based on an analysis of their light element abundance distributions, specifically using lithium as a tracer. This technique, the so-called lithium depletion boundary method (Basri, Marcy & Graham 1996; Rebolo et al. 1996; Stauffer, Schultz & Kirkpatrick 1998; Barrado y Navascués, Stauffer & Patten 1999), does however have both merits and limitations. Line strengths and elemental abundance ratios are fairly straight forward to measure, and are indeed fundamental stellar properties, perhaps more so than compared to magnetic activity indicators. Unfortunately, the strength of this technique lies in detecting lithium in M-stars and cooler, which for any group of stars at a given distance are among the faintest. Even for nearby open clusters, detecting the lithium boundary thus requires use of precious 8-10m class telescope time. Perhaps the ultimate limitation for this technique is that it is only discernibly sensitive to stars of $\lesssim$250 Myr (*e.g.,* Stauffer et al. 1998), severely limiting its widespread applicability.

The use of heavy-element abundances to establish stellar age has also been attempted, however its implementation is as yet limited. Cayrel et al. (2001) advocate using the detection of the singly-ionized uranium 238 line at 3859.6Å as an age proxy, although as they themselves note, the accuracy of this technique is currently limited by deficiencies in the nuclear data - *e.g.,* poorly-known oscillator strengths. Even with the advent of well-calibrated atomic data for uranium species, dating of open clusters using detection of stellar uranium will only be feasible for clusters older than the Hyades [600Myr], due to the prohibitively long half-lives of the two dominant naturally occurring uranium species ($\tau_{1/2} = 7.04 \times 10^8$ & 4.47×10^9 yrs for U^{235} & U^{238} respectively - CRC 2005).

Spectroscopic and photometric observations of white dwarfs, in the Galactic field and in globular and open clusters, can also yield an age estimate of the their stellar content. The detailed physics of how white dwarfs cool as they age is now well developed (Mestel 1952; Cox & Giuli 1965; Beaudet, Petrosian & Salpeter 1967), and their model-dependent cooling time-scales are well described using theoretical stellar models (Koester & Schönberner 1986; D'Antona & Mazzitelli 1989; Iben & Laughlin 1989; Wood 1992; Fontaine, Brassard & Bergeron 2001). This technique has been historically rather difficult to implement in open clusters. First, even for the nearby clusters, their white dwarf members are the faintest objects comprising the mass function, typically being fainter than V=20th magnitude (*e.g.,* Rubin et al. 2008), which is challenging for all but the largest aperture terrestrial telescopes. Second, white dwarfs are intrinsically blue objects (typically B-V$_o$ < 0.2), which until recently was problematic for capturing photons efficiently using astronomical, red sensitive spectrographs and detectors. Third, and most importantly, to properly derive the age of the cluster one must observe and characterize objects extending right down to the bottom of the white dwarf sequence; *i.e.,* those objects which are the dimmest, the coolest and hence the *old-est* white dwarfs in the cluster. Consequently, in light of such procedural difficulties, relatively few open clusters have white dwarf cooling-time age estimates available in the literature (*e.g.,* Richer et al. 1998; Bedin et al. 2005; Kalirai et al. 2003, 2005; Rubin et al. 2008).

In terms of rotation, Kawaler (1989) uses theoretical stellar spin-down models (from Kawaler 1988) to analytically derive a relationship uniquely connecting a star's B-V photometric colour and age to its period. Using a photometric colour, rotation period dataset for G & K-stars in the Hyades open cluster, he shows the Hyades rotation age to be 4.9±1.1×10^8 years. More recently, Barnes (2003, 2007 - hereafter B03, B07 respectively) exploit the morphology of photometric colour-rotation period distributions in coëval samples of stars (*e.g.,* open clusters and binary systems) to establish stellar age. In essence, this so-called *gyrochronology* technique allows one to construct rotational isochrones, in order to trace the boundaries of age dependent colour-period distributions. Crucially however, these boundary definitions further suggest the identification and coupling-state of each star's basic internal stratification in terms of their radiative zone and convection envelope.

Solar-type stars lying close to or on the *I*, or interface sequence, are probably rotating as solid bodies or close to it, and their spin-down evolution is Skumanich-like (Skumanich 1972), i.e., directly proportional to the square root of stellar age (spin-down $\propto t^{1/2}$). The most rapidly rotating solar-type stars at a given mass lie on or close to the *C*, or convective sequence. These stars are thought to be rotationally *de-coupled*; that is to say, it is likely that *only* their outer convective envelope is spinning down, with an exponential time dependency (spin-down $\propto e^{f(t)}$). Early incarnations of rotational evolution models incorporating *de-coupled* stellar structure were referred to as core-envelope (de)coupling models (*c.f.,* Endal & Sofia 1981; Stauffer et al. 1984; Soderblom et al. 1993a, Jianke & Collier Cameron 1993). Those stars which are in a transitory state between the *C* and *I*-sequences, representing a scenario whereby the outer convective envelope is *re-coupling*, probably magneto-hydrodynamically, to the inner radiative zone, constitute the so-called *gap* or *g*−stars in the gyrochronology paradigm.

Establishing stellar age for open clusters using gyrochronology models of course has its limitations. For instance for open clusters, enough stars must be photometrically monitored in order to derive rotation periods, so that a clear, well-defined distribution of interface, gap, or convective sequence objects is apparent. Such an observing programme typically requires extensive allocations of telescope time and considerable human effort. Moreover, differential rotation of solar-type stars and multiple star-spot groups on their surfaces can also introduce ambiguities into gyrochronology analyzes, since it can act to smear-out the distribution of rotation periods of a given mass.

For small samples of rotation periods in open clusters, the gyrochronology method is not applicable in multiple systems where other effects might interfere with, or even overwhelm, the regular wind-related loss of angular momentum. For instance, close binaries (*a* $\lesssim$0.1 AU) experience a tidal torque which acts to synchronize their rotation with the orbital motion of the system, in addition to any magnetic torque they experience due to stellar winds (Zahn 1989; 1994); thus, as they evolve along the main-sequence, components in the closest binaries tend to rotate faster (on average) than single stars of similar mass and age. Observations of RS CVn and BY Dra systems have shown Zahn's theoretical framework to be correct (Hall 1976; Bopp & Fekel 1977; Fekel, Moffet & Henry 1986). Binary/multiple systems must therefore be avoided, where the data allow, in estab-

lishing gyrochronology ages of stars (see Meibom, Mathieu & Stassun 2006 for a more thorough discussion).

A recent International Astronomical Union symposium (IAUS 258), dedicated to the subject of *The Age of Stars*, now provides our community with a thorough overview of an historical and modern approach to understanding the how and why of stellar ages. A careful perusal of the symposium proceedings allows, for both the novice and expert alike, a detailed insight into the theoretical framework unpinning stellar age determinations as well as the observational data calibrating and constraining such models. Of special interest to this manuscript were the oral presentations by Barnes (2009), Jeffries (2009) and Meibom (2009).

The genesis of this gyrochronology project for M 34, a $\simeq$ 200 Myr open cluster, occurred nearly ten years ago. At that epoch, SAB and GWL obtained a differential photometry dataset at Lowell Observatory over 17-nights for the Western half of the cluster, with the goal of deriving rotation periods for photometric variables in the field. The project lay dormant for some years until we noticed that Irwin et al. (2006) published new rotation period data for a sample of solar-type stars in the cluster. Unfortunately in terms of rotation, there are several fundamental problems with the Irwin et al. dataset which hamper our ability to pursue a rigorous gyrochronology analysis using their data (see § 4.4 for details). A natural progression and indeed amelioration of their period distribution analysis is to derive the gyrochronology properties of this cluster, now incorporating rotation periods derived from the differential photometry that we had obtained during the 1998 Lowell campaign. In this manuscript therefore, we now report an analysis of our differential photometry dataset for the cluster.

New BVI photometry is reported in § 3 for each photometric variable discovered in our Lowell observing campaign. Rotation periods derived from light-curve analysis of the photometric variables in our field of view are described in § 4, which includes a comparison with the Irwin et al. study. Using a clean sample of rotation periods for photometric and/or kinematic members of the M 34 cluster, we describe in § 5 how colour-period data are used in undertaking a gyrochronology analysis, which results in the derivation of the rotation age of the cluster. Also included is a commentary on how error in the gyrochronology age can be ascribed to disparate physical properties of the colour-period dataset, such as cluster non-membership, binarity and differential rotation.

2. The Open Cluster Messier 34

M 34 (NGC 1039) is a young ($\simeq$200 Myr; see Table 1) open cluster on the border of Perseus and Andromeda [RA(2000): 02^h42^m, DEC(2000): $+42^o46'$]. It is $\simeq$ 470 pc away, out of the Galactic plane [$b \simeq -16^o$], and has a reddening of E$_{B-V}$=0.07 (Canterna, Perry & Crawford 1979). These characteristics suggested to us that it would make a good target for rotation period determinations, including a derivation of its rotational age via the methodology of gyrochronology.

2.1. Extant Observations of M 34

Prior work on M 34 includes photoelectric *UBV* observations for 57 stars bluer than F3 in the M 34 field by Johnson (1954) and of 43 similar stars by Cester et al. (1977). Canterna et al. (1979) reported photoelectric photometry in Strömgren *uvby* & Hβ, for some 42 M 34 stars. Jones & Prosser (1996) published a more

extensive and deeper (down to V=16.2) survey using *BVI* CCD observations. An even deeper (V$\simeq$ 24) *VI* CCD survey has been recently published by Irwin et al. (2006). Both of the latter two studies have certain irregularities with the standardization procedures that are evident in the papers. Consequently, we use standardized photometry from a new *BVRI* survey by the Indiana group of the WIYN open cluster study (Deliyannis et al. in prep) in our analysis (see § 3).

Two proper motion surveys have been conducted in M 34. The first, by Ianna & Schlemmer (1993), has a limiting magnitude of V=14.5, and the second, by Jones & Prosser (1996), one of V=16.2. Reliable membership probabilities from these studies are limited to stars brighter than V=13.5 and V=14.5, respectively, and although >80% of the stars in our study are fainter than either of the proper motion surveys, we use them where available. Jones et al. (1997) have provided radial velocities for some 47 cluster members but few of these overlap with our photometric period sample. However, we take recourse to an on-going multi-epoch WIYN HYDRA radial velocity survey of the cluster (Meibom et al. in prep) to provide a reliable kinematic membership criterion for nearly half (25/55) of the M 34 stars for which we report new photometric periods. A thorough discussion of extant membership probabilities for M 34 stars comprising our gyrochronology sample, as well as new high resolution spectroscopic results for two photometric variables in our sample, is presented in Appendix A.

Other meritorious work on M 34 includes a study of the cluster white dwarfs by Rubin et al. (2008), who derive a minimum age of the cluster to be 64 Myr. Although Rubin et al. were not explicitly attempting an age derivation, such a result must be considered with some caution because of the lack of surety of cluster membership for their targets, the small sample size (5 objects), and the fact that only the very top of the cluster white dwarf sequence was sampled, whereby the coolest, and hence oldest white dwarfs in the cluster were not observed.

Projected equatorial rotation velocities [v sin i] for the earlier-type, higher mass stars in M 34 are provided by Ianna (1970), Hartoog (1977), and Landstreet et al. (2008), whereas for its solar-type members velocities are published by Jones et al. (1997) and Soderblom et al. (2001). For stars in common, we provide a comparison between these $v \sin i$ data and our new photometric periods in Appendix B. By removing the dual ambiguities in $v \sin i$ data (the obvious sin i factor, and the stellar radius), photometric rotation period studies far and above supersede $v \sin i$ studies - provided of course that the rotation periods are measured correctly.

Irwin et al. (2006) have provided rotation periods for some 105 stars in M 34, using photometric data obtained under considerably more restrictive conditions (observing window, and filters) than ours. Although half the stars in common between their study and our Lowell sample yield essentially the same period from multiple time-series, some discrepancies exist. A detailed comparison between their periods and ours is presented in § 4.4.

3. New Indiana CCD photometry

A new, comprehensive BVRI survey of star fields in the direction of the M 34 cluster is now available from the Indiana Group of the WIYN Open Cluster Survey (Deliyannis et al. in prep). Photometric observations of the central $40' \times 40'$ of the cluster, including $\simeq$ 100 Landolt (1992) standard stars, were obtained using the WIYN 0.9-meter telescope during the night of 24-Oct-1998. The 2048 $\times$ 2048 pixel T2KA Tekronics CCD was employed at the f/7.5 Cassegrain focus, which with its

0 $\overset{\prime\prime}{.}$68 pixel^{-1} plate scale yields an effective field of view of $\simeq 23' \times 23'$. Multiple exposures in each filter were obtained over a 2x2 mosaic for the cluster. Images were analyzed using the dedicated DAOPHOT II photometry data reduction package. Landolt standard star frames were processed using aperture photometry, whereas object frames were fitted with spatially-variable point spread functions [PSFs], and spatially-variable aperture corrections. Both the PSFs and aperture corrections were determined empirically using hundreds of isolated stars on each frame. External errors in placing instrumental magnitudes onto the standard system are < 0.02 magnitudes.

The results of the Indiana Group's photometric survey for stars relevant to this study are presented in Table 2, as well as coordinates for each star derived from SuperCosmos survey images (Hambly et al. 2001a, b; Hambly, Irwin & MacGillivray 2001). We also provide a kinematic membership assessment from an on-going survey of the cluster (Meibom et al. in prep). For two M 34 targets for which we derive a period, F4_1925 & F4_2226, there are no *B*-band photometric data available. In this instance, we rely upon a field star V−I to B−V relationship (Caldwell et al. 1993), and an assumed E_{B-V}=0.07 (Canterna et al. 1979), to transform these stars' V-Ic colours into B-V ones.

4. New Photometric Periods in M 34

4.1. Observational Programme

We initiated a differential photometry programme of observations for solar-type stars in M 34 during September-October 1998, consisting of four separate sequences of CCD images in the V and I filters, acquired respectively during a 17 night observing run (UT980929 through 981015) at Lowell Observatory, Flagstaff, Arizona, USA. The dataset consists of ∼ 60 visitations to each of two 19'×19' fields of the Western region of M 34. Each visitation typically consisted of short (**60, 40 sec**) and long (**600, 400 sec**) exposures in the V and I filters respectively, using the 2048×2048 SITe chip mounted at the Cassegrain focus of the 42inch Hall telescope of Lowell Observatory. Each field received 4-7 visitations per night in each filter, over the first 12 nights, barring UT981008 which was lost to clouds, and one visitation each on the remaining 5 nights. The time-series analysis is performed on the instrumental system with respect to chosen reference images on UT981001.

4.2. Data Analysis and Time Series Analysis:

The individual images were de-biased and flat-fielded using standard procedures in the IRAF[1] image reduction utility. Photometry for all objects on the processed images was computed via PSF fitting using DAOPHOT II and ALLSTAR II (Stetson, Davis & Crabtree 1991). Typically, we have used 50 PSF stars per image and a quadratically-varying PSF. The photometry from the individual frames was cross-matched and converted into time series using the DAOMATCH/DAOMASTER routines from Stetson (1992). These routines match stars appearing in multiple images according to user-supplied specifications, calculate the photometric offsets between frames, and output the corrected time series. The uncertainty in the frame-to-frame magnitude offsets was less than 0.001 mag for the frames

that were eventually used because of the large number (≳1000) of stars matched from frame to frame. This procedure left us with totals of ∼ 4000, ∼ 3000, ∼ 2700, and ∼ 2200 objects respectively with time series in each of the long-I, long-V, short-I and short-V exposures for the western M 34 fields.

We tested every object in the field for variability without regard to its position in a colour-magnitude diagram, or any other consideration except its intrinsic variability. Also, we performed the variability/periodicity analysis independently in each exposure time/filter combination, in order to confirm or deny it, and to calculate period error. The following procedure was adopted for each time-series file. The time series files for each field were sigma-clipped to eliminate outliers[2], and then we calculated a reduced chi square ($\tilde{\chi}^2$) for each time-series, to glean out the most variable objects. Every object with $\tilde{\chi}^2 > 3$ was subjected to a periodicity search using the CLEAN algorithm of Roberts, Lehar & Dreher (1987). The results were examined visually, and phased about reliable peaks in the power spectrum to yield phased light curves for the periodic variables. Finally, results of the (up to) four independent time-series analyzes on each object were merged together to confirm or deny the periodicity. For these stars, we calculate period errors based on multiple measurements.

As a result of the foregoing analysis, we have been able to identify forty-seven (47) objects with periods confirmed in at least two filter, exposure combinations. In addition, we derive periods for eight (8) objects for which we can only detect periodicity in one filter/exposure. The period analysis results are listed in Table 3, which also contains details of their derived periods, and standard deviations of magnitude variation in each time-series. Stars having only one period determination are assigned period errors based on the widths of the peaks in the power spectra. Phased photometric light-curves, on the instrumental system, are presented for each of our M 34 variables in Appendix C.

Our 17-night observing window allows us to detect two or more phases for all periods up to about 8.5 days. However this cut is probably too conservative, and because the slow rotators are of great interest to us, we extend our analysis to periods longer than 8.5 days. We are confident about periods as long as three quarters of the 17d baseline, i.e. ∼ 13d; however, the period errors are larger for such stars. For instance, F3_0469 (field 3) has a period of ∼ 12.9d in all 4 exposure time/filter time-series. Periods longer than our 13-day *comfort* timescale abut the sensitivity limit of our observing window, which result in consequentially larger period errors for the [2/55] systems for which we report periods >13 days (see Table 3).

4.3. Establishing Membership of M 34 from Photometric Variability Alone

Constructing a colour-magnitude diagram is the simplest way of establishing possible membership of an open cluster because stars located far from the cluster sequence are guaranteed to be non-members. Stars on the cluster sequence may or may not be *bona fide* cluster members, depending on the extent of fore- and background contamination from the Galactic field. For stars forming an apparent cluster main sequence, additional information is needed to distinguish between true members and field-star, non-member interlopers. Classical, well established

---

[2] This procedure lowers our sensitivity to eclipsing binaries and flares or other one-time variables, but has the virtue of eliminating occasional bad photometric points, which could reduce the efficacy of the period-searching software for rotational variables.

methods for member, non-member triage involve astrometric (proper motion) measurements or measuring radial velocities (*e.g.*, Stauffer 1984, Meynet et al. 1993, Perryman et al. 1998, Raboud & Mermilliod 1998, Mermilliod et al. 2008), however such measurements are not always practical to acquire. In their absence, magnetic activity (*e.g.*, X-rays) or lithium abundance indicators can be used to distinguish between cluster and non-cluster stars (*e.g.*, Prosser et al. 1995a; James & Jeffries 1997; Cargile, James & Platais 2009). Here, we propose that photometric periodicity can also be exploited to easily establish open cluster membership in a manner unbiased with respect to brightness, mass (at least for solar-type stars) and distance.

In Fig., 1, we plot colour magnitude diagrams of the cluster in BV and VI colours, along with D'Antona & Mazzitelli (1997) theoretical isochrones for 250 Myr & 470 pc in both colours. The 55 periodic variables in our Lowell fields are also identified on the figure. Photometric and/or radial velocity members, 43 in number, are flagged with red squares, whereas non-members, 12 in number, are flagged with blue circles (their periodicity and other information are tabulated in Tables 2 & 3). The cluster sequence is traced out very well by the periodic variables. In fact, in this particular case, photometric periodicity information alone provides a 78% (43/55) probability of cluster membership. We believe the reason for this behavior is that the cluster stars are younger and hence far more active and variable than the mostly older disk stars in the field. One might even envision using photometric variability to trace out cluster sequences in sparsely populated young clusters or background-dominated cluster fields.

4.4. Comparison with prior periods

Irwin et al. (2006) have published a prior study of periodic variables in M 34, and before proceeding further, we compare our periods with theirs for stars in common between the two studies. This comparison is graphically represented in Fig., 2, where symbols are assigned to stars having a varying number of independent period derivations (1-4) in our dataset. Of the 19 stars in common between the Irwin et al. sample and our own Lowell campaign, roughly half (9/19) have periods that agree within 10%. For all but two of the remaining 10 stars, Irwin et al. periods are significantly shorter than ours, where the origins for such discrepancies are not entirely clear to us.

Through comparison with an as yet unpublished photometric variability study of M 34 we can establish confidence in the Lowell campaign periods, and advocate their preferential use compared to the Irwin et al. ones. Three stars in common to the Irwin et al. study and our Lowell campaign, F3_0413, F4_0234, and F4_1147, have Meibom et al. (in prep) periods, whose photometric variability was characterized over several months worth of observation data (*e.g.,* see Meibom et al. 2009 for details of a similar observing programme for the M 35 cluster). These data, flagged stars in Fig., 2 and listed in Table 4, show that the Meibom et al. periods are an excellent match to the Lowell periods (to within 1%), whereas the Irwin et al. periods are poorly matched.

Proving the correctness of one period derivation over another is not an easy task. However, we note that our dataset has a 17-night baseline compared with the 10-night baseline of Irwin et al., suggesting that we have better sensitivity to longer period systems. Our data were also acquired all night, rather than restricted to half nights as the Irwin et al. observational data were. These facts strongly suggest that our data are less sensitive to period aliasing; indeed, several of the Irwin et al. stars lie on or

close to particular alias curves, as shown in Fig., 2. Finally, we note that most of our periods [17/19] are confirmed in at least a second filter/exposure time combination in the Lowell campaign data. Consequently, in light of the concerns that we have for aliasing effects in some of the Irwin et al. data, we will preferentially use our own periods for the remainder of this work.

5. The Photometric Period Distribution in M 34

Our rotation period distribution for photometric and/or kinematic members of M 34, as a function of intrinsic $B - V$ and $V - I$ colours, is displayed in Fig., 3. In agreement with prior results in various open clusters (B03, B07), there are no stars located in the upper left portion of the colour-period diagrams. The Sun-like [$(B-V)_o \simeq 0.64$] stars in our M 34 sample are rotating about an order of magnitude faster than the Sun. However the lower mass stars, mid-K and later, have an order-of-magnitude spread in rotation period, as has been seen before in other young open clusters. Further detailed interpretation of the M 34 colour-period diagram requires a comparison of the colour-period distributions for other young clusters.

Rotation period distributions for two comparison clusters whose ages straddle that of M 34 will allow us to critically investigate the gyrochronological properties of M 34. To this end, we display colour-period diagrams for the $\simeq$135 Myr M 35 and 600 Myr Hyades clusters in Fig., 4. Colour-period data are taken from the recent study of M 35 by Meibom et al. (2009), and for the Hyades, from Radick et al. (1987) and Prosser et al. (1995b). This side-by-side comparison shows that the ~135 Myr-old M 35 cluster has two distinct sequences of rotating stars indicated by the solid and dashed line in the figure, while the older Hyades cluster has only one. B03 called these sequences 'I' (for Interface) and 'C' (for Convective), with 'g' (for gap) stars in transition from C to I (see § 1 for a discussion of the angular momentum characteristics of CgI stars). What we see plainly from the comparison is that by the Hyades age, most rotating solar-type stars have been transformed into I-type stars. Graphs of this C-g-I transformation for a series of clusters can be found in B03 and Meibom et al. (2009).

We now take these gyrochronology sequences from the M 35 colour-period distribution, and overplot them on the M 34 data in the left hand panel of Fig., 5. This allows us to classify the gyrochronology status of the (far fewer) M 34 stars roughly, as indicated by the CgI symbols in the figure. We note that its C sequence is in the same approximate position as that of M 35, but its I sequence lies above that of M35, as expected from its older age. The manner of this inter-comparison suggests that only the stars shown in the right panel of the figure ought to be identified as I-sequence stars in M 34, which we henceforth do.

5.1. A Gyrochronology Age for M 34

It is desirable to derive an age for M 34 using our photometric period dataset, and the method of gyrochronology (B03, B07) will allow us to pursue such an analysis. This exercise will allow us to examine whether the gyro age derived is physically reasonable, and hence whether it might be usable for other clusters in future. The basis for such a gyro age calculation relies upon;

1. Deriving the true rotation period distribution of the cluster,
2. Removing possible cluster non-members, and
3. Choosing, and using only, the I-sequence stars in the cluster for the analysis.

For M 34, we have performed these three steps to the best of our ability, as described above, with the resulting set of candidate I-sequence stars in the cluster being displayed in the right-hand panel of Fig., 5. We note that the forthcoming study by Meibom et al. (in prep), which contains many more M 34 stars, will make the CgI distinction in this cluster more obvious, and verify our classifications made here. Based on fitting the open cluster colour-period distributions then available, B07 suggested that the positions of the I sequences of open clusters, or indeed that of field stars, follows the relationship;

$$P_{rot} = f(B - V).g(t) \tag{1}$$

where P_{rot}, (B-V), and t represent the measured rotation period, measured de-reddened colour, and the age respectively, and f and g are fitted functions of the stellar colour and age respectively, where he proposed that

$$f(B - V) = a(B - V - c)^b \tag{2}$$

and

$$g(t) = t^n \tag{3}$$

for which Barnes (2007) derived coefficients of $a = 0.7725 \pm 0.0110$, $b = 0.601 \pm 0.024$, $c = 0.4$, and $n = 0.5189 \pm 0.0070$. However, based on the most extensive open cluster rotation period study to date, that of M 35 by Meibom et al. (2009 - displayed in the left-hand panel of Fig., 4), the coefficients of the I-sequence fit have been recently updated to be $a = 0.770 \pm 0.014$, $b = 0.553 \pm 0.052$, and $c = 0.472 \pm 0.027$ with a fixed $n = 0.52$. However, the index n is set by the solar calibration, by demanding that the gyrochronology relationship for the I-sequence yields the solar rotation period at the solar age, the rationale for which is explained at length in B07. We note that, using their extensive rotation period dataset for M 35, Meibom et al. re-fit the colour function coefficients of Equ., 2 but did not re-fit the age exponent, n, of Equ., 3. Therefore to be mathematically rigorous, we employ the Meibom et al. (2009) a, b & c coefficients and the solar data summarized in Barnes (2007) to re-derive the $g(t)$ exponent to be $n = 0.5344 \pm 0.0015$.

Taking the Meibom et al. (2009) a, b & c coefficients and the newly derived n exponent, we fit the Equ., 1 relationship to the colour-period data of M 34 I-sequence stars, those identified in Fig., 5, in order to determine the cluster's gyro age, the one free parameter in the fit. The results of this procedure are reported in Table 5. An unweighted fit to these data yields a rotation age for M 34 to be 193 ± 9 Myr[3] ($\pm$ possible systematic errors in gyrochronology), where the quoted error is the error on the mean for these data. Such a gyro age for the cluster is consistent with the Jones & Prosser and Meynet et al. isochronal ages for M 34.

5.2. Variance of the Derived Periods about the Fit

Let us see if we can clarify the origin of items in the error budget contributing to the uncertainty in the cluster's gyrochronology age, which are in addition to any systematic error of the gyrochronology method itself. We can estimate the magnitude of the error budget by considering the additive contribution of each

star's period variance[4]. We might expect contributions to the period variance from cluster non-members, tidally-interacting binaries within the cluster, a possible age spread within the cluster, period errors, differential rotation, and finally, one from initial variations in the cluster's natal angular momentum distribution. The data listed in Table 5 show that the total period variance about the fit is ~ 43.7 days^2.

It is beyond the scope of this paper to consider possible systematic errors in the gyrochronology method, which is calibrated using both the Sun and a selection of young open clusters with measured photometric periods. An understanding of this error will probably require another decade of rotational work on open clusters. It would be unsurprising if such a study eventually identified a 15-20% systematic error in the application of gyrochronology to real colour-period samples.

The cluster colour-magnitude diagrams (see Fig. 1) suggest that 3 periodic field variables could have sneaked into our 43 member star sample had we not had the radial velocity measurements to reject them. This suggests that of our 22 purely photometrically chosen members (see Table 3), one possibly two are non-members, making this unlikely to be any significant contributor to the error. The mean variance contributor of any given star in our M 34 period sample is 1.68 days^2 (see Table 5), which means that non-member variance contribution from photometric members is at most $\simeq 3.4$ days^2 ($\sim 8\%$ of the variance total). Of the 26 candidate I-sequence stars in M 34, twelve of them are classified as photometric-only members of the cluster, *i.e.,* having no kinematic classification (with a mean period variance of 2.33 days^2). Of these twelve, only three have noticeably large period variances (F4_1357, 7.84 days^2; F4_1007, 5.76 days^2; F3_0664, 4.41 days^2). In any case contribution to period variance, and hence gyro age errors, by cluster non-members is at a low level.

There is also a possibility that some scatter in the gyro ages for individual M 34 stars is contributed by systems in tidally locked binaries, which will be addressed in greater detail in the Meibom et al. (in prep) study. We note that of the candidate I-sequence stars reported in Table 5, 14/24 have kinematic classifications. Only one of these stars is a binary system, with no data being available as to whether it is tidally-locked or not. On average, one such data point would contribute 1.68 days^2 to the total variance, or $\sim 4\%$.

Observational studies of other young open clusters and associations suggest that they are cöeval to within about a few Myr (*e.g.,* Wichmann et al. 2000; Palla & Randich 2005; James et al. 2006). While spreads in observed quantities that also change with age are generally believed to originate in other ways, we note that recent theoretical work by Baraffe, Chabrier & Gallardo (2009) shows that as a phenomenon, episodic accretion onto young solar-type stars can also act to introduce a luminosity spread, and hence age spread, in the main sequence loci of Hertzsprung Russell diagrams. An intrinsic age spread of 10Myr (*e.g.,* Jeffries 2009) at B-Vo colours of 0.60, 1.00 & 1.40 in our 193Myr gyrochronology fit yields a maximum period variance of only 0.1 days^2. Such an intrinsic internal age spread within the cluster will therefore not contribute any significant variance.

---

[3] Using all of the Meibom et al. (2009) coefficients, including $n = 0.52$, a resultant gyrochronology age for M 34 of 223 ± 11 Myr would be obtained.

[4] We define each star's period variance as (Measured Period - Fitted Period)^2, where the measured period is the photometric variability period determined from our differential photometry and the fitted period is that derived from Equ 1, using dereddened B-V colours, an assumed mean gyro age of 193 Myr and the Meibom et al. (2009) a, b, c coefficients, with an n exponent, $n = 0.5344 \pm 0.0015$.

Inspection of Fig. 5 and Table 3 shows that photometric period errors are quite large for the longer periods in our sample. We attribute this effect to the 17-night baseline of observations and expect that these errors will decline with a longer baseline dataset, such as the forthcoming Meibom et al. (in prep) sample. Indeed, an informal comparison shows that they will be able to define the cluster's I-sequence better than our dataset allows. Another indication of this is that M 34 I-sequence stars with smaller periods errors are, in general, located closer to the fitted sequence (see Fig. 6). Based solely on the period measurement errors themselves (see Table 5), the variance contribution due to imprecise period measurement is $\simeq 15.5$ days^2 (35.5% of the total).

Differential rotation must be present in this sample, in the sense that two stars with the same equatorial velocity might present spot groups at observed at different latitudes, introducing some period scatter in the observations. We do not however expect this to contribute much to the observed variance, based on the parametrization of its contribution to the fractional period variance via $\delta P/P = 10^{-1.85}P^{0.3}$, following the analysis in Donahue, Saar & Baliunas (1996) and Barnes (2007). For the I-sequence stars listed in Table 5, this effect contributes only something like $\simeq 2.06$ days^2 to the variance, equivalent to 5% of the total variance budget.

This leaves a remainder variance of 21.1 days^2 (48% of the total) to be accounted for by the effects of either; (a) the systematic difference between the gyro fit and the observation data, or (b) the residual influence of initial variations. Because these two contributors have differing dependencies on cluster and observational parameters, it should be possible to understand their separate contributions as the rotation period database of open cluster stars expands.

6. Discussion and Summary

We have presented the results of a 17-night differential photometry campaign over the Western half of the central region of the open cluster M 34. For all photometrically variable stars, we construct differential photometry light-curves, from which we derive periodicity. It is assumed that the photometric variability of objects consistent with cluster membership is due to the presence of magnetic-field induced starspots on their surfaces, rotating with the star; the derived periods are therefore representative of the angular velocity of the star.

In order to assess cluster membership, we exploit an extensive standardized CCD survey of the cluster, which shows that the majority of photometric variable stars [47/55] lie along the loci of the cluster main sequence in V/B-V and V/V-I space. Moreover, we are able to confirm kinematic membership of the cluster for 21 stars from an on-going radial velocity survey of the cluster (Meibom et al. in prep), 5 of which show radial velocity variations (multiple systems). Four (4) of the photometric variables are kinematic non-members. Stars which are either photometric or kinematic non-members were excluded from the gyrochronology analysis.

We note the existence of another photometric period dataset for solar-type stars in the M 34 cluster (Irwin et al. 2006). We present an analysis comparing periods for stars in common between our Lowell campaign and their study. We detail several concerns that we have with the integrity of their dataset, notably their short observing window (< 10 nights) and their half-night observing cadence. After having verified that several Irwin et al. periods are most likely measurement aliases, and that our

Lowell campaign periods agree those derived from an independent, separate, long time base-line differential photometry survey, we preferentially employ our period results in pursuing a gyrochronology age analysis for this cluster.

Rotation periods for *bona fide* cluster members, in concert with photometric B-V colours, are used to create colour-period distributions, from which we outline a specific methodology for performing a gyrochronology analysis. In order to calculate the actual gyrochronology age of the cluster, we assign each M 34 member its CgI status, as judged from its position in the colour-period diagram. I-sequence stars in M 34 are classified specifically as those objects in the colour-period diagram lying above the I-sequence locus of the younger M 35 cluster, yielding a mean gyro age for all I-sequence stars in M 34 of 193 ± 9 Myr.

There are two existing sets of age determination for the M 34 cluster, using the traditional isochrone fitting method and the white dwarf cooling time-scale. Together with gyrochronology, all three methods suffer from various forms of dependency on stellar models under-pinning their theoretical frameworks. Furthermore, both the isochrone fitting and white dwarf methods suffer from a dependence on (or an assumption of) cluster distance, while gyrochronology is free from distance as an input parameter.

The isochronal age of M 34 is not that well defined (see § 2 & Table 1), with a broad range in determined values. Unfortunately, the lack of observed giants in the cluster, and its broad *turn-off* locus in the V/B-V colour magnitude diagram precludes a precise assessment of its isochronal age. Based on existing studies, the mean isochronal age of the cluster is 250 ± 67 Myr.

The white dwarf cooling time-scale age for M 34 is also problematic because its result is based upon only five (5) objects whose membership of the cluster is not yet confirmed. Furthermore, the terminus of the white dwarf sequence has not yet been observed. In simple terms, the faintest, coolest, and therefore oldest white dwarfs have yet to be characterized, and the cluster's cooling time-scale age of 64.0 ± 12.9 Myr (Rubin et al. 2008) must be considered as a lower limit.

We conclude by noting that a study of M 34 by Meibom et al., including both a multi-month differential photometry campaign and also a multi-year radial velocity membership and binarity campaign, similar to their prior work in M 35, is in preparation. Their survey will yield several hundred new photometric periods of M 34 solar-type stars, the I- and C-sequences of which should be far more clearly defined than they are from our Lowell campaign results. Their dataset should allow them to better define the gyrochronology age of M 34, and we await their results eagerly.

References

Baraffe, I., Chabrier, G., & Gallardo, J., 2009, ApJL, 702, L27
Barnes, S. A. 2003, ApJ, 586, 464 [B03]
Barnes, S. A. 2007, ApJ, 669, 1167 [B07]
Barnes, S. A. 2009, *The Ages of Stars*, proceedings of the International Astronomical Union Symposium, eds E. E. Mamajek, D. R. Soderblom, & R. F. G. Wyse, Vol 258, p.345: Cambridge University Press
Barrado y Navascués, D., Stauffer, J. R., & Patten, B. M. 1999, ApJ, 522, L53
Barry, D. C., Cromwell, R. H., Hege, K., & Schoolman, S.A. 1981, ApJ, 247, 210
Basri, G., Marcy, G., & Graham, J. 1996, ApJ, 458, 600

Beaudet, G., Petrosian, V., & Salpeter, E. E., 1967, ApJ, 150, 979

Bedin, L. R., Salaris, M., Piotto, G., King, I. R., Anderson, J., Cassisi, S., & Momany, Y., 2005, ApJ, 624, 45

Bopp, B. W., & Fekel, F. C. 1977, AJ, 82, 490

Caldwell, J. A. R., Cousins, A. W. J., Ahlers, C. van Wamelen, P., & Maritz, E. J. 1993, South African Astronomical Observatory Circulars, Vol 15, P1

Canterna, R., Perry, C. L., & Crawford, D. L. 1979, PASP, 91, 263

Cargile, P A., James , D. J., & Platais, I., 2009, AJ, 137, 3230

Cayrel, R., Hill, V., Beers, T. C., Barbuy, B., Spite, M., Spite, F., Plez, B., Andersen, J., Bonifacio, P., Francois, P., Molaro, P., Nordström, B., & Primas, F., 2001, Nature, 409, 691

Cester, B., Giuricin, G., Mardirossian, F., & Pucillo, M., 1977, A&AS, 30, 227

Cox, J. P., & Giuli, R. T., 1965, *Principles of Stellar Structure*, New York: Gordon & Breach

CRC Handbook of Chemistry and Physics, 86th edition, 2005, Boca Raton: Taylor & Francis

D'Antona, F., & Mazzitelli, I. 1989, ApJ, 347, 934

D'Antona, F., & Mazzitelli, I. 1997, *Memorie della Societa Astronomica Italiana*, Vol. 68, P.807

Demarque, P. R., & Larson, R. B., 1964, ApJ, 140, 1544

Demarque, P. R., & Gisler, G. R., 1975, A&AS, 201, 237

Donahue, R. A., Saar, S. H. & Baliunas, S. L., 1996, ApJ, 466, 384

Donati, J.F., et al. 1997, MNRAS, 291, 658

Endal, A. S., & Sofia, S. 1981, ApJ, 243, 625

Fekel, F. C., Moffet, T. J., & Henry, G. W. 1986, ApJS, 60, 551

Fontaine, G., Brassard, P., & Bergeron, P., 2001, PASP, 113, 409

Giampapa, M. S., Hall, J. C., Radick, R. R. & Baliunas, S. L., 2006, ApJ, 651, 444

Gray, D. F., 1992, *The Observation and Analysis of Stellar Photospheres* 2nd edn, Cambridge: University Press

Hall, D. S. 1976, *Periodic Variable Stars*, W. Fitch, Dordrecht: Reidal, 1976, 287

Hambly, N.C., et al. 2001a, MNRAS, 426, 1279

Hambly, N. C., Davenhall, A. C., Irwin, M. J., & MacGillivray, H. T., 2001b, MNRAS, 326, 1315

Hambly, N.C., Irwin, M. J., & MacGillivray, H. T., 2001c, MNRAS, 326, 1295

Hartoog, M. R., 1977, ApJ, 212, 723

Henry, T. J., Soderblom, D. R., Donahue, R. A., & Baliunas, S. L. 1996, AJ, 111, 439

Ianna, P. A., 1970, PASP, 82, 825

Ianna, P. A., & Schlemmer, D. M. 1993, AJ, 105, 209

Iben, Jr, I., & Laughlin, G., 1989, ApJ, 341, 312

Irwin, J., et al. 2006, MNRAS, 370, 954

James, D. J., & Jeffries, R. D., 1997, MNRAS, 291, 252

James, D. J., Melo, C., Santos, N., & Bouvier, J., 2006, A&A, 446, 971

Jeffries, R. D., 2009, *The Ages of Stars*, proceedings of the International Astronomical Union Symposium, eds E. E. Mamajek, D. R. Soderblom, & R. F. G. Wyse, Vol 258, p.95: Cambridge University Press

Jianke, L., & Collier Cameron, A., 1993, MNRAS, 261, 766

Johnson, H. L., 1954, ApJ, 119, 185

Jones, B. F., & Prosser, C. F. 1996, AJ, 111, 1193

Jones, B.F., Fischer, D., Shetrone, M., & Soderblom, D.R., 1997, AJ, 114, 352

Kalirai, J. S., Fahlman, G. G., Richer, H., & Ventura, P., 2003, AJ, 126, 1402

Kalirai, J. S., et al. 2005, ApJ, 618, 123

Kawaler, S. D., 1988, ApJ, 333, 236

Kawaler, S. D., 1989, ApJ, 343, 65

Koester, D., & Schönberner, D., 1986, A&A, 154, 125

Landolt, A. U., 1992, AJ, 104, 340

Landstreet, J. D., Silaj, J., Andretta, V., Bagnulo, S., Berdyugina, S. V., Donati, J.-F., Fossati, L., Petit, P., Silvester, J., & Wade, G. A., 2008, A&A, 481, 465

Maggio, A., et al. 1987, ApJ, 315, 687

Mamajek, E., & Hillenbrand, L., 2008, ApJ, 687, 1264

Meibom, S., 2009, *The Ages of Stars*, proceedings of the International Astronomical Union Symposium, eds E. E. Mamajek, D. R. Soderblom, & R. F. G. Wyse, Vol 258, p.357: Cambridge University Press

Meibom, S., Mathieu, R., & Stassun, K., 2006, ApJ, 653, 621

Meibom, S., Mathieu, R., & Stassun, K., 2009, ApJ, 695, 679

Mengel , J. G., Sweigart, A. V., Demarque, P. R., & Gross, P. G., 1979, ApJS, 40, 733

Mermilliod, J.-C., Grenon, M., Platais, I., James, D. J., & Cargile, P. A., 2008, A&A, 485, 95

Mestel, L., 1952, MNRAS, 112, 583

Meynet, G., Mermilliod, J.-C., & Maeder, A. 1993, A&AS, 98, 477

Naylor, T., 2009, MNRAS, 399, 432

Table 1. Extant isochronal ages for M 34

Method	Stellar Age [Myr]	Reference
UBV	100	Cester et al. (1977)
uvby	500	Canterna et al. (1979)
UBV	250	Ianna & Schlemmer (1993)
UBV	180	Meynet et al. (1993)
BVIc	200-250	Jones & Prosser (1996)

Noyes, R. W., Hartmann, L. W., Baliunas, S. L., Duncan, D. K., & Vaughan, A. H., 1984, ApJ, 279, 763

Palla, F., & Randich, S., *The Initial Mass Function 50 Years Later*, INAF Osservatorio Astrofisico di Arcetri, Firenze, Italy, 2005, Astrophysics and Space Science Library Vol 327, Springer, Dordrecht, edited by E. Corbelli & F. Palle, p.73

Perryman, M. A. C., Brown, A. G. A., Lebreton, Y., Gómez, A., Turon, C., Cayrel de Strobel, G., Mermilliod, J.C., Robichon, N., Kovalevsky, J., & Crifo, F., 1998, A&A, 331, 81

Prosser, C. F., Stauffer, J. R., Caillault, J-P., Balachandran, S., Stern, R. A., & Randich, S., 1995a, AJ, 110, 1229

Prosser, C. F., Shetrone, M. D., Dasgupta, A., Backman, D. E., Laaksonen, B. D., Baker, S. W., Marschall, L. A., Whitney, B. A., Kuijken, K., & Stauffer, J. R., 1995b, PASP, 107, 211

Raboud, D., & Mermilliod, J.C. 1998, A&A, 329, 101

Radick, R. R., Thompson, D. T., Lockwood, G. W., Duncan, D. K., & Baggett, W. E. 1987, ApJ, 321, 459

Rebolo, R., Martín, E. L., Basri, G., & Zapatero-Osorio, M. R. 1996, ApJ, 469, L53

Richer, H. B., Fahlman, G. G., Rosvick, J., & Ibata, R., 1998, ApJ, 504, 91

Roberts, D. H., Lehar, J., & Dreher, J. W., 1987, AJ, 93, 968

Rubin , K. H. R., Williams, K. A., Bolte, M., & Koester, D., 2008, AJ, 135, 2163

Sandage, A., 1958, *Ricerche Astronomiche*, Vol. 5, Specola Vaticana, Proceedings of a Conference at Vatican Observatory, Castel Gandolfo, May 20-28, 1957, Amsterdam: North-Holland, and New York: Interscience, 1958, edited by D.J.K. O'Connell., p.41

Skumanich, A. 1972, ApJ, 171, 565

Soderblom, D.R., Duncan D.K., & Johnson, D. R. H. 1991, ApJ, 375, 722

Soderblom, D.R., Stauffer, J. R., MacGregor, K. B., & Jones, B. F. 1993a, ApJ, 409, 624

Soderblom, D.R., Jones, B.F., Balachandran, S., Stauffer, J. R., Duncan, D.K., Fedele, S.B., & Hudon, J.D., 1993b, AJ, 106, 1059

Soderblom, D.R., Stauffer, J. R., Hudon, J.D., & Jones, B.F., 1993c, Ap&SS, 85, 315

Soderblom, D.R., Jones, B. F. & Fischer, D., 2001, ApJ, 563, 334

Stauffer, J. R., 1984, ApJ, 280, 189

Stauffer, J. R., Hartmann, L. W., Soderblom, D.R., & Burnham, N. 1984, ApJ, 280, 202

Stauffer, J. R., Schultz, G., & Kirkpatrick, J. D. 1998, ApJ, 499, L199

Stetson, P. B., Davis, L. E., and Crabtree, D. R., 1991, in *CCDs in Astronomy*, ed. G. Jacoby, ASP Conf. Series, 8, p. 282.

Stetson, P. B., 1992, in *Stellar Photometry - Current Techniques and Future Developments*, eds. C. J. Butler & I. Elliot, IAU colloq. 136, p. 291

Wichmann, R., Torres, G., Melo, C. H. F., Frink, S., Allain, S., Bouvier, J., Krautter, J., Covino, E., & Neuhäuser, R., 2000, A&A, 359, 181

Wilson, O. C. 1963, ApJ, 138, 832

Wilson, O. C. 1964, PASP, 76, 28

Wilson, O. C. 1966, Science, 151, 1487

Wilson, O. C., & Skumanich, A. 1964, ApJ, 140, 1401

Wood, M. A., 1992, ApJ, 386, 539

Zahn, J.-P. 1989, A&A, 220, 112

Zahn, J.-P. 1994, A&A, 288, 829

Zombeck, M. V. 1990, *Handbook of Space Astronomy and Astrophysics*, 2nd edn, Cambridge: University Press

Table 2. Astrometry, photometry and membership assignments are presented for those M 34 stars for which photometric periods are derived in the Lowell campaign.

Internal[a] Identifier	RA[b] (J2000)	DEC[b] (J2000)	JP 96[c]	V[d]	Verr[d]	B-V[d]	B-Verr[d]	V-I[d]	V-Ierr[d]	Phot[e] Mem	RV[e] Mem
F3_0172	02 41 05.141	+42 56 43.202	JP 49	14.584	0.017	0.881	0.023	0.956	0.024	Yes	Yes-sing
F3_0176	02 41 36.611	+42 50 20.288	JP 167	14.659	0.009	0.888	0.013	1.051	0.013	Yes	Yes-sing
F3_0215	02 41 00.981	+42 52 46.695	JP 41	14.918	0.010	0.944	0.015	1.039	0.014	Yes	Yes-sing
F3_0258	02 42 02.552	+42 51 51.721	JP 289	15.236	0.009	1.017	0.013	1.118	0.013	Yes	Yes-sing
F3_0306	02 41 57.472	+43 00 26.530	JP 265	15.503	0.014	1.061	0.019	1.262	0.027	Yes	Yes-bin
F3_0320	02 41 37.557	+42 57 21.593	JP 172	15.664	0.017	1.116	0.025	1.237	0.024	Yes	
F3_0383	02 40 49.882	+42 55 31.520		16.179	0.017	1.230	0.025	1.424	0.024	Yes	Yes-sing
F3_0430	02 41 50.490	+42 58 10.016		16.424	0.013	1.309	0.019	1.505	0.018	Yes	Yes-sing
F3_0469	02 40 49.090	+42 48 20.648		16.604	0.018	1.353	0.030	1.550	0.025	Yes	
F3_0485	02 41 06.638	+42 48 22.011		16.732	0.010	1.355	0.016	1.619	0.014	Yes	
F3_0487	02 40 44.889	+42 53 47.221		16.818	0.020	1.348	0.030	1.701	0.027	Yes	
F3_0600	02 41 18.447	+42 58 21.342		17.394	0.020	1.522	0.035	1.863	0.027	Yes	
F3_0664	02 41 20.454	+42 58 52.278		17.862	0.022	1.511	0.057	1.999	0.029	Yes	
F4_0136	02 41 47.384	+42 43 38.525	JP 213	13.151	0.010	0.614	0.014	0.718	0.015	Yes	Yes-sing
F4_0169	02 41 04.952	+42 46 51.343	JP 50	13.510	0.010	0.668	0.014	0.786	0.014	Yes	Yes-sing
F4_0194	02 41 28.142	+42 38 37.095	JP 133	13.662	0.010	0.722	0.014	0.805	0.015	Yes	Yes-sing
F4_0234	02 41 33.429	+42 42 11.625	JP 148	13.959	0.010	0.768	0.014	0.844	0.014	Yes	Yes-sing
F4_0303	02 41 49.932	+42 37 13.906	JP 227	14.366	0.009	0.837	0.013	0.912	0.013	Yes	Yes-sing
F4_0317	02 41 49.354	+42 36 37.613	JP 224	14.410	0.010	0.875	0.014	0.959	0.014	Yes	Yes-sing
F4_0327	02 41 44.167	+42 46 07.333	JP 199	14.483	0.009	0.883	0.013	0.941	0.013	Yes	Yes-sing
F4_0335	02 41 35.247	+42 41 02.323	JP 158	14.546	0.010	0.860	0.014	0.994	0.014	Yes	Yes-bin
F4_0450	02 41 23.098	+42 40 15.954	JP 113	14.960	0.010	0.965	0.014	1.058	0.014	Yes	Yes-sing
F4_0667	02 41 06.187	+42 46 20.783	JP 52	15.623	0.009	1.100	0.013	1.233	0.013	Yes	Yes-bin
F4_0695	02 41 42.922	+42 33 13.910	JP 197	15.643	0.021	1.156	0.030	1.289	0.029	Yes	Yes-sing
F4_0730	02 40 49.647	+42 46 54.799	JP 18	15.741	0.017	1.121	0.025	1.257	0.024	Yes	
F4_0736	02 40 48.542	+42 39 25.716		15.844	0.021	1.078	0.028	1.328	0.029	Yes	Yes-bin
F4_0803	02 41 50.301	+42 44 37.371	JP 229	16.025	0.010	1.234	0.014	1.373	0.013	Yes	Yes-sing
F4_0804	02 41 48.974	+42 39 59.680		16.034	0.010	1.176	0.015	1.378	0.014	Yes	
F4_0852	02 41 53.246	+42 35 26.394		16.294	0.009	1.225	0.013	1.634	0.013	Yes	Yes-bin
F4_0942	02 41 46.371	+42 32 32.128		16.341	0.020	1.268	0.029	1.498	0.028	Yes	
F4_1007	02 40 50.752	+42 41 19.844		16.839	0.022	1.510	0.033	1.901	0.034	Yes	
F4_1020	02 40 36.693	+42 41 32.500		16.608	0.021	1.330	0.031	1.584	0.030	Yes	
F4_1055	02 40 42.791	+42 38 59.153		16.639	0.021	1.342	0.031	1.600	0.029	Yes	
F4_1147	02 41 43.854	+42 45 07.859		17.009	0.010	1.406	0.017	1.749	0.013	Yes	
F4_1315	02 40 53.997	+42 38 48.513		17.347	0.022	1.441	0.036	1.815	0.030	Yes	
F4_1357	02 41 44.198	+42 35 36.074		17.476	0.011	1.450	0.021	1.911	0.015	Yes	
F4_1369	02 41 51.600	+42 29 50.864		17.496	0.015	1.513	0.027	1.934	0.021	Yes	
F4_1392	02 41 38.851	+42 43 01.148		17.654	0.011	1.504	0.025	1.963	0.015	Yes	
F4_1566	02 41 31.131	+42 41 14.283		18.132	0.012	1.549	0.032	2.137	0.016	Yes	
F4_1617	02 41 26.292	+42 30 15.124		18.165	0.027	1.570	0.064	2.178	0.035	Yes	
F4_1793	02 41 20.042	+42 39 23.652		18.606	0.015	1.393	0.063	2.285	0.019	Yes	
F4_1925[f]	02 41 21.947	+42 32 32.637		19.040	0.037	1.577	0.045	2.350	0.045	Yes	
F4_2226[f]	02 40 31.108	+42 40 25.105		19.659	0.067	1.625	0.071	2.626	0.071	Yes	

Table 2. continued.

Internal Identifier	RA (J2000)	DEC (J2000)	JP 96	V	Verr	B-V	B-Verr	V-I	V-Ierr	Phot Mem	RV Mem
F3_0071	02 40 44.422	+42 54 04.516		12.855	0.019	1.047	0.025	1.153	0.026	No	
F3_0121	02 41 47.414	+42 50 09.223	JP 212	13.741	0.009	1.248	0.013	1.354	0.013	No	
F3_0163	02 41 55.003	+42 52 53.485	JP 258	14.440	0.008	0.900	0.011	0.986	0.012	Yes	No
F3_0165	02 41 51.794	+42 46 20.473	JP 244	14.419	0.008	0.865	0.011	0.956	0.011	Yes	No
F3_0388	02 41 38.227	+42 55 43.112	JP 174	15.952	0.010	0.975	0.015	1.076	0.022	No	
F3_0413	02 41 48.478	+42 49 33.840	JP 218	16.242	0.010	1.143	0.015	1.412	0.014	Yes	No
F3_0437	02 40 48.970	+42 56 12.434		16.022	0.018	0.647	0.025	0.748	0.025	No	
F3_0692	02 40 57.994	+42 49 44.614		17.136	0.010	0.857	0.016	1.061	0.015	No	
F3_2310	02 40 44.085	+42 53 58.059		99.999	9.999	9.999	9.999	9.999	9.999		
F4_0167	02 41 48.825	+42 31 31.702	JP 223	13.502	0.021	0.938	0.026	1.030	0.031	No	
F4_0404	02 41 27.663	+42 35 42.306	JP 131	14.730	0.010	0.852	0.014	0.932	0.014	Yes	No
F4_0515	02 41 27.188	+42 43 41.881	JP 129	15.111	0.010	0.903	0.014	0.977	0.014	No	

$a-$ Identifier format is XX_YYYY, where 'XX' are representations F3 and F4 for targets detected on M 34 western Field 3 or western Field 4 images, and 'YYYY' are internal catalog numbers.

$b-$ Astrometric data are derived from coordinate matches in the SuperCosmos survey catalogs (Hambly et al. 2001a, b, c).

$c-$ JP 96 identifiers are for photometric variables which are correlated with Jones & Prosser (1996) sources

$d-$ BVI photometric data are taken from the Indiana Group survey (*c.f.,* § 3).

$e-$ Membership assignments are based upon whether a target star lies on (or close to) the V/B-V and/or V/V-I main sequence loci [see Fig., 1] or whether a target star has a radial velocity consistent with the cluster's systemic velocity (Meibom et al. in prep; see also § 2.1 and Meibom et al. 2006).

$f-$ B-V colours are determined using a field star V-I to B-V relationship (Caldwell et al. 1993), assuming $E_{V-I} = 1.25 \times E_{B-V}$, and $E_{B-V}=0.07$ (Canterna et al. 1979).

Table 3. Photometric periods and ancillary data are presented, resulting from the light-curve analysis of variable stars detected in the Lowell M 34 fields.

Internal[a] Identifier	Data[b] Epochs	Sigma Clipped[c] StdDev [mags]	Period [days]	B-V$_o^d$	Mem[e]
F3_0172-lIIVsV	53/54/59	0.00883/0.01010/0.01190	8.0 ± 1.0	0.811	Y;Ys
F3_0176-lIIVsIsV	53/54/58/59	0.04275/0.06460/0.04313/0.06427	2.780 ± 0.005	0.818	Y;Ys
F3_0215-lIIVsIsV	52/54/58/59	0.01121/0.01722/0.01439/0.02020	7.47 ± 0.11	0.874	Y;Ys
F3_0258-lIIVsV	53/54/58	0.01182/0.01250/0.01457	11.0 ± 1.0	0.947	Y;Ys
F3_0306-lIsIsV	53/58/59	0.01886/0.01809/0.02081	1.1435 ± 0.0007	0.991	Y;Yb
F3_0320-lIIVsV	52/54/58	0.00898/0.01023/0.01430	8.511 ± 0.001	1.046	Y;
F3_0383-lIIV	52/54	0.00776/0.00937	9.5 ± 0.4	1.160	Y;Ys
F3_0430-lV	54	0.01253	10.5 ± 1.0	1.239	Y;Ys
F3_0469-lIIVsIsV	52/54/57/57	0.01344/0.01745/0.01768/0.02225	12.9 ± 0.3	1.283	Y;
F3_0485-lIIV	52/54	0.01040/0.01393	12.0 ± 1.0	1.285	Y;
F3_0487-lIIV	53/54	0.01076/0.01388	8.4 ± 0.6	1.278	Y;
F3_0600-lIIV	53/54	0.01263/0.02503	7.44 ± 0.05	1.452	Y;
F3_0664-lI	52	0.01077	10.5 ± 1.0	1.441	Y;
F4_0136-sIsV	60/60	0.01457/0.01794	2.87 ± 0.03	0.544	Y;Ys
F4_0169-lIIVsIsV	55/42/60/59	0.01275/0.01297/0.01094/0.01429	3.81 ± 0.08	0.598	Y;Ys
F4_0194-sIsV	60/60	0.00817/0.00889	2.20 ± 0.03	0.652	Y;Ys
F4_0234-lIIVsV	54/55/60	0.00692/0.00984/0.01014	5.56 ± 0.07	0.698	Y;Ys
F4_0303-lIIVsIsV	55/55/60/60	0.00800/0.00941/0.00839/0.00978	7.4 ± 0.3	0.767	Y;Ys
F4_0317-lIIVsIsV	55/55/59/60	0.01701/0.02159/0.01698/0.02167	6.8 ± 0.1	0.805	Y;Ys
F4_0327-lVsV	55/60	0.01471/0.01406	7.6 ± 1.1	0.813	Y;Ys
F4_0335-lIIVsIsV	55/55/60/60	0.01538/0.01953/0.01601/0.02032	0.89 ± 0.02	0.790	Y;Yb
F4_0450-lIIVsIsV	54/55/60/60	0.00985/0.01181/0.01264/0.01368	8.00 ± 0.21	0.895	Y;Ys
F4_0667-lIIVsV	54/55/59	0.01122/0.01819/0.02028	7.97 ± 0.05	1.030	Y;Yb
F4_0695-lI	54	0.00748	4.3 ± 0.5	1.086	Y;Ys
F4_0730-lIIVsIsV	55/55/60/59	0.02944/0.04619/0.03109/0.04695	8.41 ± 0.10	1.051	Y;
F4_0736-lIIVsIsV	55/55/60/60	0.01875/0.02715/0.02022/0.02911	0.786 ± 0.001	1.008	Y;Yb
F4_0803-lVsI	55/60	0.01435/0.01416	12.6 ± 0.7	1.164	Y;Ys
F4_0804-lIIVsIsV	55/55/60/60	0.02568/0.04152/0.02448/0.04239	4.95 ± 0.04	1.106	Y;
F4_0852-lIIVsIsV	55/55/59/60	0.01547/0.02368/0.01624/0.02564	0.879 ± 0.002	1.155	Y;Yb
F4_0942-lIIVsV	54/55/60	0.00942/0.01300/0.02362	9.4 ± 0.3	1.198	Y;
F4_1007-lIIV	55/55	0.00774/0.01177	15 ± 2	1.440	Y;
F4_1020-lIIVsIsV	55/55/60/59	0.01344/0.01846/0.01568/0.02528	8.6 ± 0.4	1.260	Y;
F4_1055-lIIVsIsV	55/55/60/60	0.01427/0.02542/0.02233/0.02664	6.80 ± 0.15	1.272	Y;
F4_1147-lV	55	0.01883	0.589 ± 0.001	1.336	Y;
F4_1315-lIIV	54/54	0.01429/0.01913	12.2 ± 0.5	1.371	Y;
F4_1357-lIIV	55/55	0.01197/0.01973	9.4 ± 0.2	1.380	Y;
F4_1369-lIIV	53/53	0.01886/0.02578	11.85 ± 0.13	1.443	Y;
F4_1392-lIIV	55/55	0.01496/0.02385	6.5 ± 0.5	1.434	Y;
F4_1566-lIIV	55/54	0.01920/0.03248	11.2 ± 0.1	1.479	Y;
F4_1617-lV	52	0.03379	7.3 ± 0.5	1.500	Y;
F4_1793-lIIV	55/53	0.02221/0.04966	7.5 ± 0.6	1.323	Y;
F4_1925-lV[f]	44	0.09210	12.7 ± 2.0	1.507	Y;
F4_2226-lI[f]	55	0.02681	6.0 ± 0.5	1.555	Y;
F3_0071-sIsV	58/59	0.02052/0.02502	3.014 ± 0.008	0.977	N;
F3_0121-lVsV	54/59	0.00851/0.00881	8.4 ± 0.2	1.178	N;
F3_0163-lIsIsV	53/58/59	0.00814/0.00943/0.00935	14 ± 2	0.830	Y;N
F3_0165-lI	52	0.01089	12 ± 1	0.795	Y;N
F3_0388-lIIVsIsV	53/54/58/59	0.01534/0.02141/0.01715/0.02448	11.59 ± 0.01	0.905	N;
F3_0413-lIIVsIsV	53/54/58/59	0.01640/0.02417/0.01909/0.02982	5.45 ± 0.08	1.073	Y;N
F3_0437-lIIVsV	53/54/59	0.00859/0.01134/0.01563	9.7 ± 0.4	0.577	N;
F3_0692-lIIV	53/54	0.01886/0.02686	0.3368 ± 0.0001	0.787	N;
F3_2310-lIIV	52/54	0.02667/0.02846	2.991 ± 0.008	- - -	
F4_0167-lIIVsI	54/55/59	0.01321/0.01091/0.00961	9.2 ± 0.9	0.868	N;
F4_0404-lIIVsV	55/55/60	0.01099/0.01419/0.01461	6.6 ± 0.3	0.782	Y;N
F4_0515-lIIVsV	55/55/60	0.00886/0.00957/0.01239	8.2 ± 0.1	0.833	N;

a− Internal Identifiers are the same as those detailed in Table 2. Designations indicating exposure time and filter choice for a given light-curve are annotated. For instance, *lI* represents *long-I*, for light-curves derived from long exposures in the I-filter. Thus, *lIIVsIsV* represents four independent light-curves created from image sequences of 400seconds, I-filter; 600seconds, V-filter; 40seconds, I-

filter & 60seconds, V-filter, respectively (namely, long-I, long-V, short-I & short-V).

$b-$ Number of photometric data points in each light-curve, derived from each target's image series, in a given filter and exposure time sequence.

$c-$ For each target's light-curve, in a filter+exposure combination, standard deviations of the differential magnitudes are provided. The time series files for each target were sigma-clipped to eliminate outliers. A Δ-magnitude for each light-curve can be determined by multiplying these standard deviations by $2\sqrt{2}$ (strictly speaking this is only true for perfectly sinusoidal variations).

$d-$ E_{B-V}=0.07 is adopted; Canterna et al. (1979)

$e-$ Abridged cluster membership criteria are reproduced from Table 2, with format Photometric; Kinematic (s-single, b-binary).

$f-$ B-V colours are determined using a field star V-I to B-V relationship (Caldwell et al. 1993), assuming $E_{V-I} = 1.25\times E_{B-V}$, and E_{B-V}=0.07.

Table 4. A comparison of photometric periods for three M 34 stars common to the Lowell campaign, the Irwin et al. study and the Meibom et al. (in prep) study (*c.f.,* Fig., 2 and § 4.4).

ID	Lowell [days]	Irwin et al. [days]	Meibom et al. [days]
F3_0413	5.45 ± 0.08	2.458	5.47
F4_0234	5.56 ± 0.07	0.822	5.47
F4_1147	0.589 ± 0.001	1.429	0.592

Table 5. Gyrochronological ages for I-sequence stars in M 34

Identifier	JP[a] no.	# of periods derived[b]	(B-V)o	Measured Period [days]	Gyro Age[c] [Myr]	Fitted[d] Period [days]	Period[e] Variance [days^2]
F4_0136	JP 213	2	0.544	2.87 ± 0.03	178.5 ± 3.5	2.99	0.0144
F4_0169	JP 50	4	0.598	3.81 ± 0.08	170.0 ± 6.7	4.08	0.0729
F4_0234	JP 148	3	0.698	5.56 ± 0.07	188.4 ± 4.4	5.63	0.0049
F4_0303	JP 227	4	0.767	7.4 ± 0.3	244.1 ± 18.6	6.5	0.81
F4_0317	JP 224	4	0.805	6.8 ± 0.1	183.8 ± 5.0	7.0	0.04
F4_0327	JP 199	2	0.813	7.6 ± 1.1	220.9 ± 59.8	7.1	0.25
F3_0172	JP 49	3	0.811	8.0 ± 1.0	244.6 ± 57.2	7.0	1.00
F3_0215	JP 41	4	0.874	7.47 ± 0.11	180.4 ± 5.0	7.74	0.0729
F4_0450	JP 113	4	0.895	8.00 ± 0.21	194.5 ± 9.6	7.96	0.0016
F3_0258	JP 289	3	0.947	11.0 ± 1.0	313.1 ± 53.3	8.5	6.25
F4_0667	JP 52	3	1.030	7.97 ± 0.05	145.0 ± 1.7	9.28	1.7161
F3_0320	JP 172	3	1.046	8.511 ± 0.001	159.3 ± 0.1	9.429	0.84272
F4_0730	JP 18	4	1.051	8.41 ± 0.10	154.4 ± 3.4	9.47	1.1236
F3_0383		2	1.160	9.5 ± 0.4	162.2 ± 12.8	10.4	0.81
F4_0803	JP 229	2	1.164	12.6 ± 0.7	273.5 ± 28.5	10.5	4.41
F4_0942		3	1.198	9.4 ± 0.3	150.4 ± 9.0	10.7	1.69
F3_0430		1	1.239	10.5 ± 1.0	174.8 ± 31.2	11.1	0.36
F3_0485		2	1.285	12.0 ± 1.0	211.3 ± 33.0	11.4	0.36
F3_0469		4	1.283	12.9 ± 0.3	242.5 ± 10.6	11.4	2.25
F4_1315		2	1.371	12.2 ± 0.5	196.4 ± 15.1	12.1	0.01
F4_1357		2	1.380	9.4 ± 0.2	119.3 ± 4.8	12.2	7.84
F3_0664		1	1.441	10.5 ± 1.0	137.2 ± 24.5	12.6	4.41
F4_1369		2	1.443	11.85 ± 0.13	171.7 ± 3.5	12.61	0.5776
F4_1566		2	1.479	11.2 ± 0.1	148.8 ± 2.5	12.9	2.89
F4_1007		2	1.440	15.0 ± 2.0	267.8 ± 66.8	12.6	5.76
F4_1925		1	1.507	12.7 ± 2.0	183.0 ± 53.9	13.1	0.16

a− *JP* identifier from Jones & Prosser (1996).

b− Number of filter/exposure combinations yielding photometric period derivations for a given star.

c− Gyro ages determined using Meibom et al. (2009) I-sequence colour function coefficients, *viz* $a = 0.770 ± 0.014$, $b = 0.553 ± 0.052$ & $c = 0.472 ± 0.027$, and an age function exponent $n = 0.5344 ± 0.0015$ (see § 5.1).

d− Assuming a mean gyrochronology age for M 34 of 193Myr (the mean of the ages calculated in column 6 - see § 5.1) and the Meibom et al. (2009) coefficients, with $n = 0.5344 ± 0.0015$, we use intrinsic (B-V) colours and Equ.,1 to derive a fitted period for each M 34 I-sequence star.

e− Each star's contribution to the period variance [(Measured Period - Fitted Period)^2] is noted, where the total variance is 43.73 days^2, with a mean of 1.68 days^2.
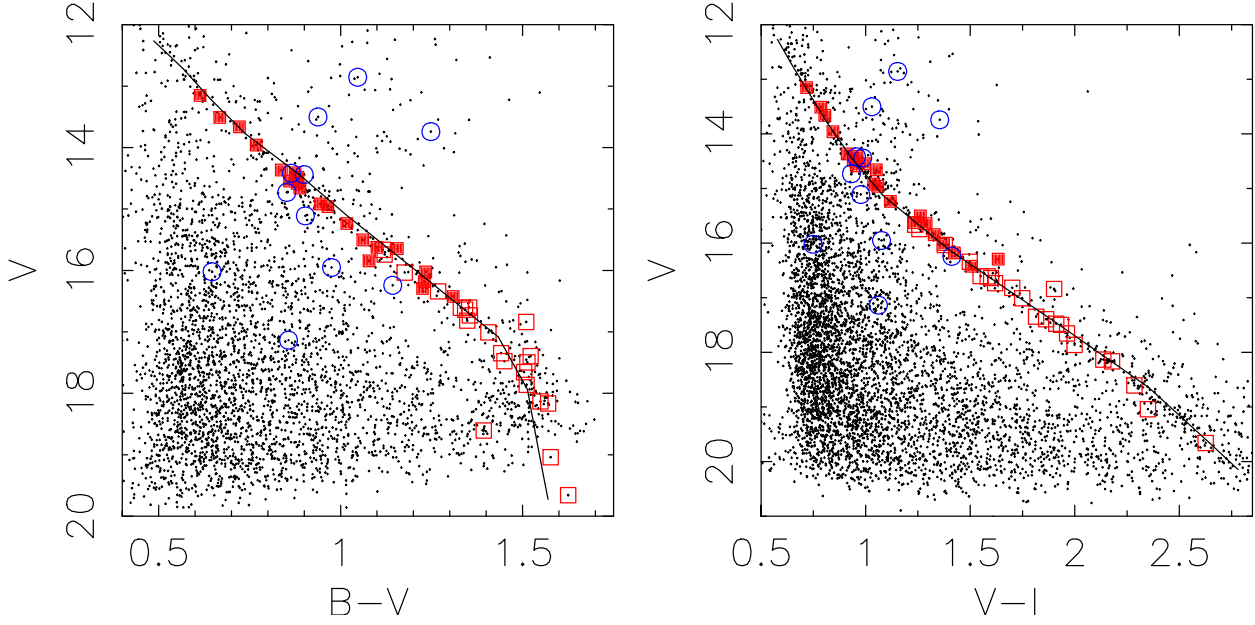
Fig. 1. Colour magnitude diagrams, in B-V and V-I colours, are presented for the entire photometry catalogue of the M 34 BVIc survey conducted by the Indiana Group. Solid lines represent D'Antona & Mazzitelli (1997) theoretical isochrones, for a cluster age of 250 Myr, a distance of 470pc, and assuming $E_{V-I} = 1.25 \times E_{B-V}$, and E_{B-V}=0.07 (Canterna et al. 1979). Red squares, highlighting photometric and radial velocity members of the cluster (solid symbols), and photometric cluster membership only (open symbols) are plotted for M 34 stars for which we have derived photometric periods during the Lowell campaign. Blue circles depict those other periodic photometric variables in the field of M 34 which are photometric and/or radial velocity non-members of the cluster.
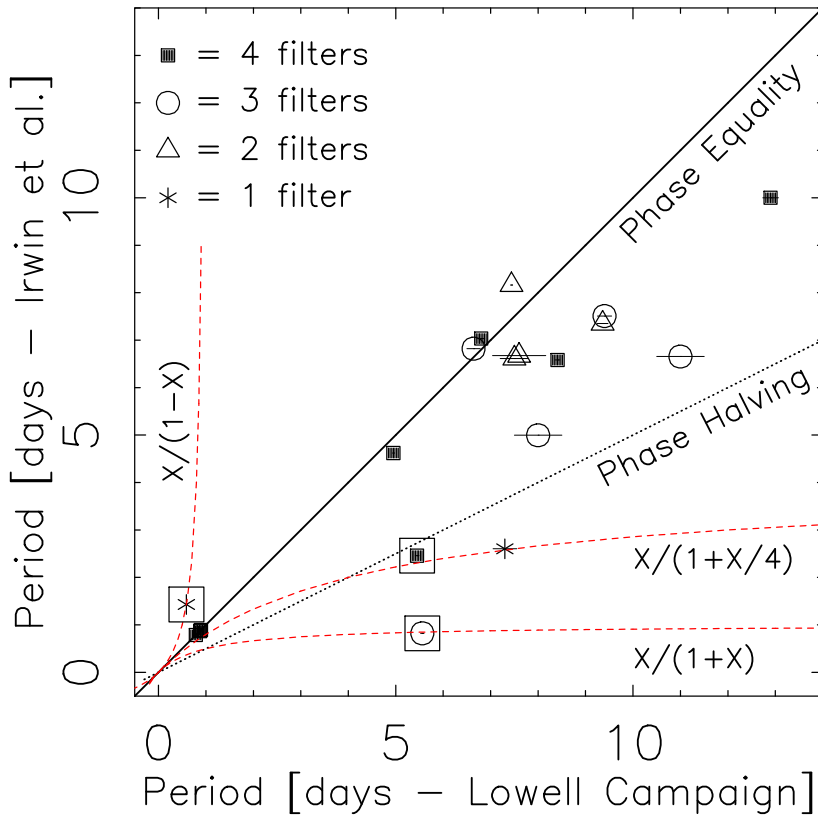
Fig. 2. Photometric periods for M 34 stars common to our Lowell campaign and the Irwin et al. study are shown. Periods determined from the Lowell campaign, using photometric light-curves in up to four (4) different filter/exposure time combinations, are depicted by the filled-square, circle, triangle and asterisk symbols (see Tables 2 & 3). We include error bars on our Lowell periods, which for many targets are smaller than the symbol sizes. No error bars are available for the Irwin et al. periods. The solid line represents equality between the two studies, and is not a fit to the data. The dotted line represents phase-halving while the dashed lines represent several period-aliasing loci, respectively. About one-third of the sample have equal period determinations (within the errors). Of the remainder, all but two of the Irwin et al. periods are shorter than ours. See text for possible reasons for the discrepancy (see § 4.4). The three flagged stars [with boxed symbols] are discrepant ones where our periods have been confirmed by a forthcoming Meibom et al. (in prep) study.
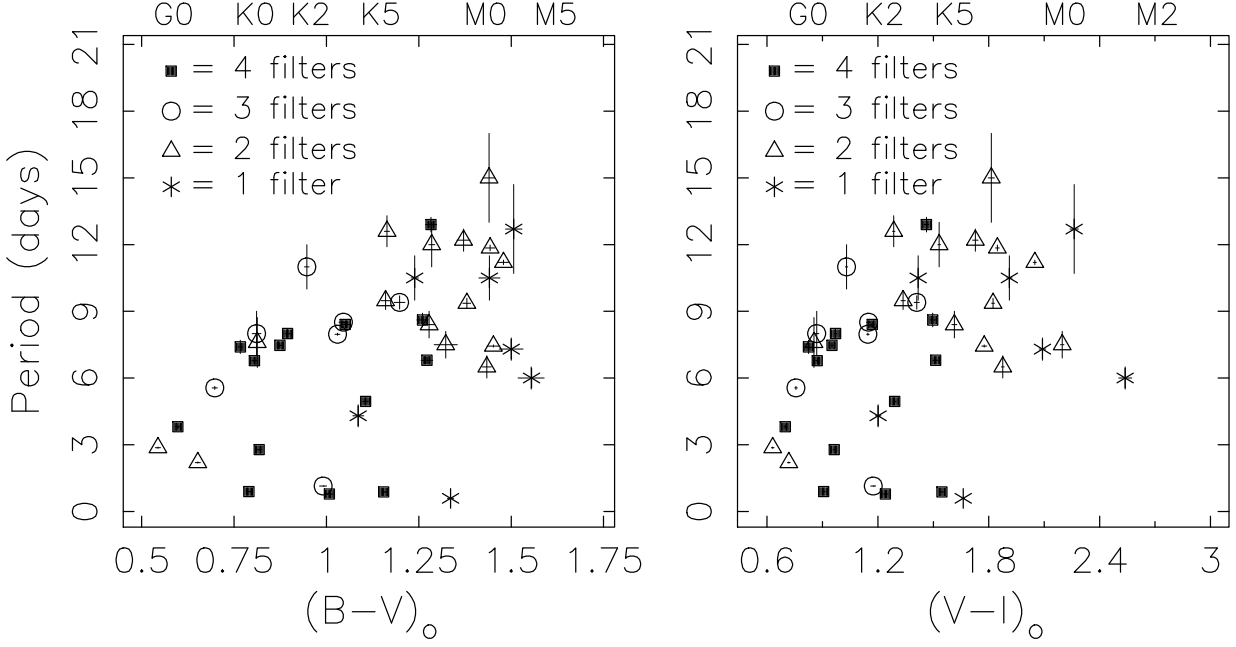
Fig. 3. Photometric period distributions, as a function of intrinsic colours (B-V)$_o$ and (V-I)$_o$, are plotted for solar-type stars in NGC 1039 (M 34). We adopt E$_{B-V}$=0.07 (Canterna et al. 1979), and E$_{V-I}$ = 1.25× E$_{B-V}$. Period symbols are the same as those depicted in Fig., 2. Error bars are included, and are for some targets smaller than the symbol sizes. Approximate spectral types for a given colour are annotated on the upper abscissae (from Zombeck 1990).
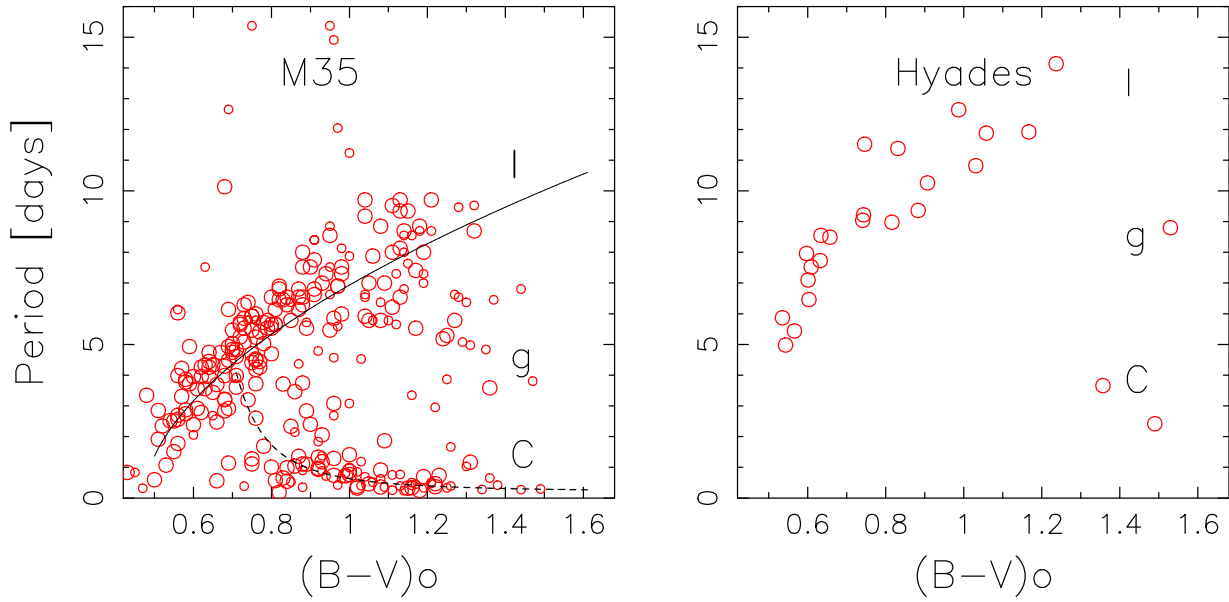
Fig. 4. In the left-hand panel, the rotation period distribution (in days) of the ≃135 Myr M 35 cluster is plotted against intrinsic (B-V) colour (data from Meibom et al. 2009); stars which are both photometric and kinematic members of the cluster are plotted with larger symbols than stars having photometric membership alone. Over-plotted are 135 Myr interface [solid line] and convection [dashed line] gyrochronology loci from the calibration by Meibom et al. (2009). In the right-hand panel, similar colour-period data are plotted for the 600 Myr Hyades cluster (data from Radick et al. 1987; Prosser et al. 1995b). Under the paradigm of gyrochronology, specific regions of the colour-period distributions are identified with C [convective], g [gap] and I [interface] symbols.
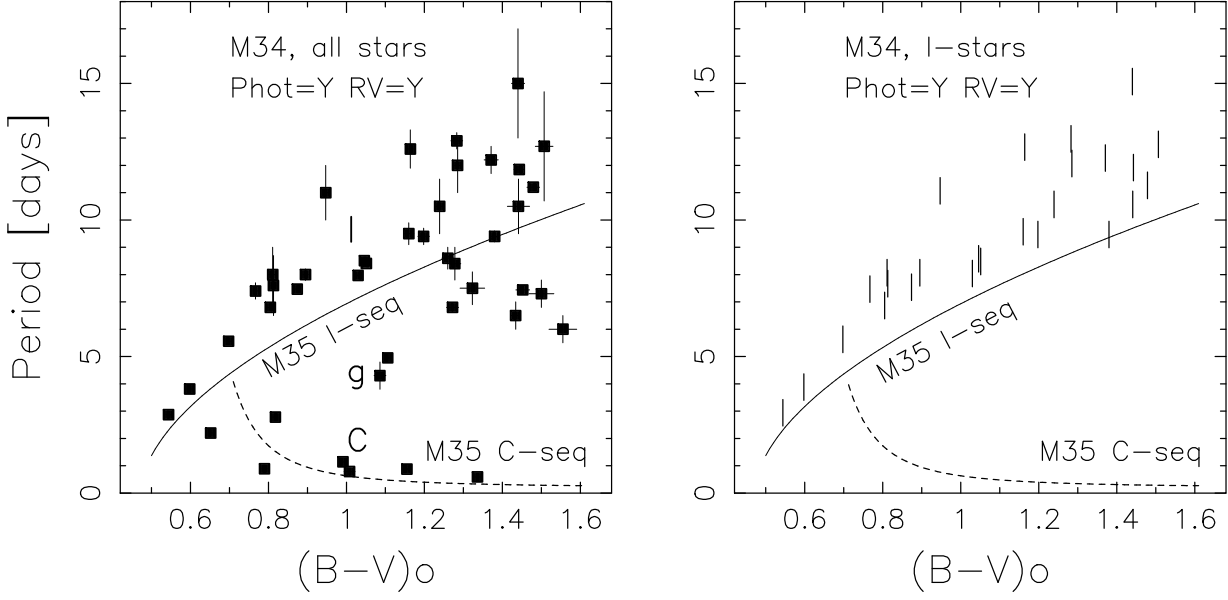
Fig. 5. The colour-period distribution for all photometric and/or kinematic members of M 34 (see Table 3) is plotted in the left hand panel. Over-plotted are gyrochronology Interface and Convection sequence loci (solid & dashed lines respectively) for the 135 Myr M 35 cluster (Barnes 2003, Meibom et al. 2009). Regions of the colour-period diagram where approximately 200 Myr stars, classified as Interface, gap and Convective status in gyrochronology space, are identified with I, g or C symbols respectively. Candidate Interface sequence stars in the M 34 cluster, lying above the Meibom et al. M 35 Interface sequence, are identified as I-symbols in the right-hand panel; see § 5 for details.
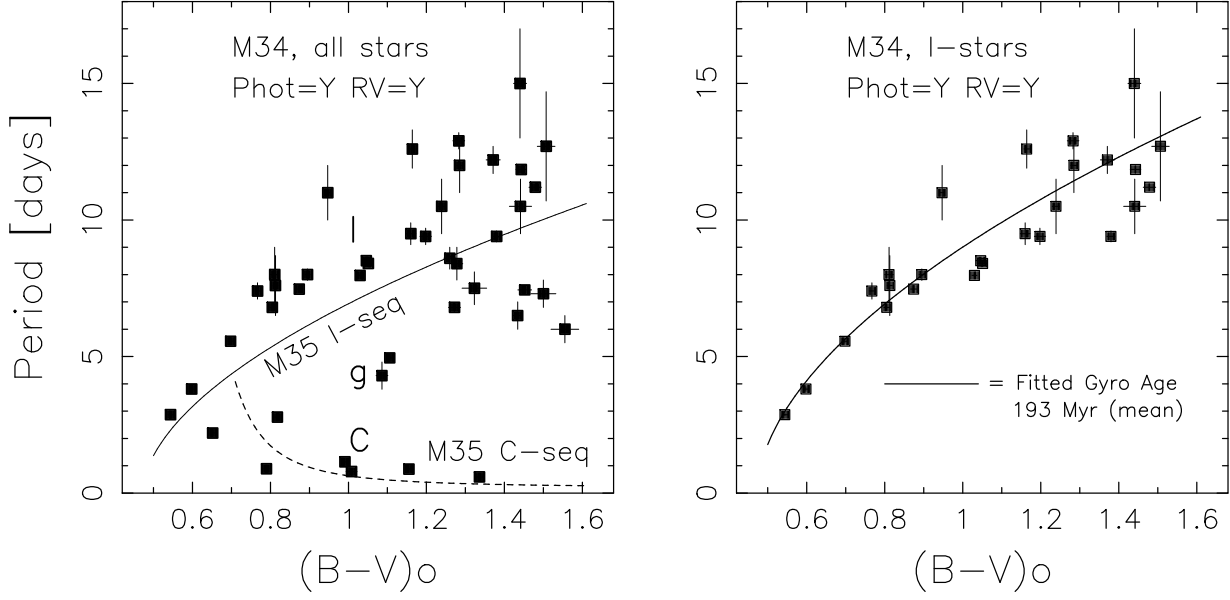
Fig. 6. This figure, very similar to Fig., 5, shows the colour-period data for our M 34 candidate I-sequence stars. The additional solid line in the right-hand panel represents the mean gyrochronology age of the I-stars in M 34 (193 Myr - see Table 5). This new gyrochronology I-sequence is calculated using updated colour-function coefficients (see Equ.,1-3 and Meibom et al. 2009) together with our new derivation of the $g(t)$ exponent ($n = 0.5344$ - see Equ., 3).

Appendix A: Cluster Membership of M 34 Using Extant Kinematic Measurements

There exist two extant kinematic studies of the M 34 cluster which can assist us further in establishing cluster membership for our gyrochronology sample. The first, by Jones & Prosser (1996), relies upon 2-d space motions in the form of proper motions, although their high-fidelity membership probabilities are magnitude limited to about V≃ 14.5. While JP96 proper motion results do extend to fainter magnitudes, their reliability reduces. That is to say, a fainter M 34 star with a 00% proper motion probability may indeed still be a *bona fide* member of the cluster, insomuch as Poisson-limited proper motion errors could lead to erroneously lower proper motion probabilities.

The second, by Jones et al. (1997), employing 1-d heliocentric radial velocities, can be used to establish cluster membership, or in the very least, establish cluster non-membership (or binarity). Unfortunately neither membership probabilities nor velocity errors were reported by Jones et al., however we can exploit their measurements in our membership assessment (see below). Interestingly, in the same manuscript, Jones et al. report Li I 6708Å equivalent widths [EWs] for their target stars. Even though the detection of lithium in solar type stars is not a requisite for cluster membership, its absence is almost ubiquitous among the generally older, Galactic field stars. The very presence of a substantial lithium line in solar-type stellar spectra is in itself indicative of youth (<< 1000 Myr; *e.g.,* Soderblom et al. 1993b, James & Jeffries 1997, James et al. 2006).

For each of the M 34 stars in our sample, we have collated these additional membership criteria published by JP96 and Jones et al. (1997) in Table A.1. Its Lowell identifier is listed in column 1 in concert with its JP96 identifier in column 2. Each star's photometric and radial velocity membership flag, reproduced from Tables 2 & 3, are cited in columns 3 & 4 respectively, whereas a flag confirming the detection of lithium 6708Å in its spectrum (from Jones et al. 1997) is listed in column 5. Corresponding Jones et al. radial velocities are detailed in column 6, as well as their associated membership probabilities in column 7 (see below and Fig. A.1). V-band magnitudes of each star are listed in column 8 and finally, cluster membership probabilities based on the proper motions reported in JP96 are reproduced in column 9.

In the first instance, we note that all stars in common between our gyrochronology sample and the Jones et al. sample have a significant lithium detection, indicative of stellar youth. These stars are therefore unlikely to be field star interlopers, which when combined with the photometric membership criterion, can safely be considered as *bona fide* cluster members. In the second, the radial velocity data from Jones et al. study do seem to cluster around -10km s^{-1}, however, specific membership assignments are difficult to assess due to the associated scatter in the individual measurements. In order to understand whether the scatter in these radial velocities is due to a true dispersion in the data or is an admixture of single and binary member measurements, together with cluster non-members, we have constructed a histogram for all radial velocities published in the Jones et al. survey. This histogram, plotted in Fig. A.1, clearly shows a peak in the distribution representing the cluster's systemic heliocentric radial velocity. In order to investigate the dispersion about the central peak, we fit an unweighted Gaussian function to the velocity histogram, noting that the fit does not include background contamination due to binarity or cluster non-members, and assumes that the sample is complete. The Gaussian function is centred on −12.49 km s^{-1} with a 1σ width of 2.32 km s^{-1}, which

we can exploit to determine a membership probability (reported in column 7 of Table A.1) for each individual star based on its radial velocity and these Gaussian fit parameters.

A.1. Results:

Analysis of the additional membership data reported in Table A.1 yields few surprises. Of all the Lowell periodic variables identified as photometric and/or RV members in Table 2, only two of them, F3_0172 & F3_0215, have a zero probability of being proper motion members according to the JP96 survey. Interestingly however, their V-magnitudes lie right at the point at which the JP96 proper motions begin to become less reliable due to Poisson-error limits on their photographic plate measurements, which brings their validity into question. Furthermore, we have noted in § 5.2 that the gyrochronology sample may indeed suffer from contamination due to one or two cluster non-members masquerading as *bone fide* members, but we argue that their contribution to the period variance, and hence gyro errors, is small. In fact, F3_0172 & F3_0215 contribute a combined period variance of 0.79 days^2, which is only a 1.8% effect (see Table 5). In spite of their low contribution to the period variance, we remain in the uncomfortable position of choosing whether to include these photometric and kinematic members of the cluster in our gyrochronology sample, or to exclude them on the basis of their proper motion membership probabilities. In order to further assess their cluster membership status, we have recently obtained high resolution optical spectra of these two stars using the Canada France Hawai'i Telescope [CFHT], the analysis of which we discuss below (see § A.2).

Finally, all bar one of the Jones et al. (1997) stars are radial velocity members of the cluster, which correlates well with our own radial velocity data. The one Jones et al. star, F4_0136, that is formally a cluster non-member based on a Gaussian probability fit to their radial velocity data plotted in Figure A.1, actually shows up as a single cluster star member in the long term synoptic velocity survey of Meibom et al. (in prep - see also § 2.1). Curiously, over the 9-epochs of observation covering 2.5-years, that Meibom et al. have for this star, its varies about *their* average radial velocity of -8.0 km s^{-1} by only 0.68 km s^{-1}. Interestingly, a Gaussian fit to all radial velocities for the 70 single and binary M 34 stars for which Meibom et al. have obtained results yields a cluster systemic velocity of −7.59 ± 1.02 km s^{-1}. Assuming the Jones et al. velocity is not in error, this star may be a binary member of the cluster, albeit with either a long-period orbit or a considerably eccentric one.

A.2. Cluster Membership Status for stars F3_0172 & F3_0215:

Two stars exhibiting variability in our differential photometric survey of the M 34 cluster, for which we derive periods, namely F3_0172 & F3_0215, present us with somewhat of a conundrum. While these stars have photometric and radial velocity properties consistent with cluster membership, with relatively short photometric periods indicative of youth (compared to the Galactic field), and result in gyrochronology ages appropriate for a 200 Myr group of stars, they possess proper motion vectors incongruent with the remainder of the cluster. In an attempt to establish or refute genuine cluster membership for these two objects, we have recently observed them at high resolution using the fibre-fed, bench-mounted ESPaDOns échelle spectrograph, located in a Coudé-like instrument chamber in the CFHT

Observatory. The primary goal of these observations is to detect lithium at 6708Å, and measure its equivalent width in these stars, thereby confirming their relative youth and increasing their probability of being *bona fide* cluster members.

During the evening of 27 January 2010, high resolution (R≃ 60, 000) spectra were acquired for stars F3_0172 & F3_0215 using the fibre-fed ESPaDOns spectrograph, in service with the 3.6-m Canada France Hawai'i Telescope located on top of Mauna Kea, Hawai'i, USA. The ESPaDOns spectrograph consists of a 79 lines mm^{-1} échelle grating imaged onto a 2048 × 4608 EEV CCD detector, having 13.5 μm square pixels, with photon input delivered by separate 100 μm (1.6 arcsec) diameter sky and target fibres. This set-up yields a FWHM of cross correlated ThAr arc lines of 0.271Å at 6700Å, and a complete wavelength range of 3699 → 10481Å. Using this set-up, F3_0172 & F3_0215 were observed for exposures totalling 2000 & 2140 seconds respectively, resulting in spectra with S/N≃ 20 at 6700Å.

For each of the targets, we exploit our CFHT ESPaDOns spectra in order to measure their heliocentric radial velocity and their Li I 6708Å EW. The removal of CCD instrumental effects, as well as the extraction of wavelength-calibrated spectra, have been achieved by two independent data reduction methodologies. In the first, we performed the bias-subtraction, flat-fielding, spectral order tracing, optimal extraction and wavelength calibration using standard IRAF procedures. In the second, we used the direct output from Libre-ESpRIT (Donati et al. 1997), the dedicated pipeline software for the ESPaDOns spectrograph. A cross-match of radial velocities and EWs for each target from the two reduction methods reassuringly yields consistent results to within ±0.1 km s^{-1} and ±3mÅ respectively.

Heliocentric radial velocities were derived, relative to the well-exposed standard star HD 32963, in the spectral region of the Mg triplet lines (5104 → 5176Å). Cross correlation of HD 32963 with other radial velocity standard stars observed during the CFHT programme shows that the zero-point in placing our velocities onto the standard system is ≃0.2 km s^{-1}. The relatively low S/N of our target spectra results in radial velocity precision errors of ≃0.5 km s^{-1}.

In order to measure equivalent widths for the Li I 6708Å line in our targets, each spectrum between 6586 → 6711Å, was normalized using continuum fitting after spectra extraction. Each EW was calculated using both the direct integration and the Gaussian fitting methods, whose values were within a few percent of each other. In the lithium region, Li I EWs include contributions from the small Fe I+CN line at 6707.44 Å, leading to measured Li I EWs which are representative of a slightly (10−20 mÅ) over-estimated photospheric Li presence. Soderblom et al. (1993b) report that this Fe line blend has an EW = [20(B-V)$_0$ - 3]mÅ, determined through an empirical relationship for main sequence, solar-type stars. For each target star, we removed the Fe I line contribution before transforming Li I EWs into abundances, N(Li) - on a scale where log N(H)=12, using the effective temperature-colour (B−V) relation from Soderblom et al (1993c), and the curves of growth presented in Soderblom et al. (1993b). Data products, radial velocity and lithium measurements, from the CFHT spectroscopic observations of F3_0172 & F3_0215 are presented in Table A.2.

CFHT radial velocities of F3_0172 & F3_0215 are consistent with cluster membership of M 34 irrespective of whether we compare their individual values to the Jones et al. (1997) sample or to the Meibom et al. (in prep) one. For the Jones et al. sample, their kinematic membership probabilities are non-zero although they are quite low at 08% & 03% (for F3_0172 & F3_0215 respectively). Their membership probabilities are far more convincing when compared to the Meibom et al. sample (with respective values of 79% & >99%).

The lithium content of both F3_0172 & F3_0215 is substantial indicating that these stars are relatively young compared to the general Galactic field, whose solar-type stellar content is typically old and has had sufficient time to have proton-burned considerable fractions of its natal lithium. In order for these stars to be judged as likely members of the M 34 cluster, not only must they contain lithium in their atmospheres, but it must quantitatively fit into the mass-dependent lithium abundance distribution for the cluster. In Figure A.2, we plot the lithium abundances for F3_0172 & F3_0215 that we have determined from our CFHT spectra in concert with the extant mass-dependent lithium distribution for M 34 stars (data taken from Jones et al. 1997, who employed identical (B-V)$_o$-Temperature, Fe I line correction and lithium curves of growth as we have used). It is clear that both F3_0172 & F3_0215 have lithium abundances consistent with the mass-dependent lithium distribution of the M 34 cluster, and must be considered lithium abundance members.

JP96 proper motion vectors for F3_0172 & F3_0215 indicate cluster non-membership. However their V-magnitudes render JP96 2-d kinematic membership probabilities questionable, because at or about this magnitude, JP96 proper motion accuracy and precisions begin to have strong dependencies on the Poissonian errors of their centroiding measurements. In consideration that these two stars are both photometric and kinematic members of the cluster, have photometric periods consistent with the remainder of the cluster's distribution, and have measured lithium abundances which lie right along the trend of the mass-dependent lithium distribution for the cluster, they are probable M 34 cluster members and we retain them in our gyrochronology sample.

Table A.1. Cluster membership assessments for Jones & Prosser (1996) stars in our period sample.

Internal[a] Identifier	JP96[b]	Phot[a] Mem	RV[a] Mem	Li Mem[c] J97	RV J97[c] [km/s]	RV Mem[d] J97	V[a] [mag]	PM Prob[e] JP96
F3_0172	JP 49	Y	Ys	...	...	...	14.584	00%
F3_0176	JP 167	Y	Ys	...	...	...	14.659	44%
F3_0215	JP 41	Y	Ys	...	...	...	14.918	00%
F3_0258	JP 289	Y	Ys	Y	-10.8	Y (47%)	15.236	76%
F3_0306	JP 265	Y	Yb	Y	-17	Y (5%)	15.503	53%
F3_0320	JP 172	Y	...	Y	-9.8	Y (25%)	15.664	03%
F4_0136	JP 213	Y	Ys	Y	-5.7	N (0%)	13.151	94%
F4_0169	JP 50	Y	Ys	...	...	...	13.510	04%
F4_0194	JP 133	Y	Ys	Y	-11.8	Y (77%)	13.662	96%
F4_0234	JP 148	Y	Ys	...	...	...	13.959	05%
F4_0303	JP 227	Y	Ys	Y	-15.4	Y (21%)	14.366	92%
F4_0317	JP 224	Y	Ys	Y	-9.4	Y (18%)	14.410	91%
F4_0327	JP 199	Y	Ys	Y	-9.0	Y (13%)	14.483	85%
F4_0335	JP 158	Y	Yb	Y	-9.9	Y (26%)	14.546	86%
F4_0450	JP 113	Y	Ys	Y	-13.5	Y (67%)	14.960	84%
F4_0667	JP 52	Y	Yb	...	...	...	15.623	26%
F4_0695	JP 197	Y	Ys	...	...	...	15.643	05%
F4_0730	JP 18	Y	...	...	...	...	15.741	36%
F4_0803	JP 229	Y	Ys	Y	-9.9	Y (26%)	16.025	46%
F3_0121	JP 212	N	...	...	...	...	13.741	00%
F3_0163	JP 258	Y	N	...	...	...	14.440	00%
F3_0165	JP 244	Y	N	...	...	...	14.419	00%
F3_0388	JP 174	N	...	...	...	...	15.952	00%
F3_0413	JP 218	Y	N	...	...	...	16.242	17%
F4_0167	JP 223	N	...	...	...	...	13.502	00%
F4_0404	JP 131	Y	N	...	...	...	14.730	00%
F4_0515	JP 129	N	...	...	...	...	15.111	00%

a− Data taken from Tables 2 & 3.
b− *JP* identifier from Jones & Prosser (1996).
c− Cluster membership based on radial velocities and lithium 6708Å equivalent widths, taken from Jones et al. (1997) [J97].
d− Radial velocity membership assessments are based on a Gaussian fit to the entire Jones et al. (1997) radial velocity sample (see also Fig. A.1).
e− Proper motion membership probabilities are taken from JP96.

Table A.2. CFHT spectroscopic data products for M 34 candidate members F3_0172 & F3_0215.

Internal[a] Identifier	JP96[b]	(B-V)$_o^a$	Temp[c] [K]	HJD[d] [(+2450000)]	RV [km s^{-1}]	Li I + Fe I [e] EW [mÅ]	Fe I [f] EW [mÅ]	Li I 6708Å[g] EW [mÅ]	N(Li)[h]
F3_0172	JP 49	0.811	5139	5223.713	-8.4	115	13	102	2.003
F3_0215	JP 41	0.874	4946	5223.712	-7.4	153	14	139	1.985

a− Data taken from Tables 2 & 3.
b− *JP* identifier from Jones & Prosser (1996).
c− Temperature determined from (B-V)$_o$ relationship in Soberblom et al. (1993c - equ. 3)
d− HJD - heliocentric julian date
e− Equivalent width measurement, by Gaussian fitting, of the blended Li I and Fe I 6708Å lines.
f − Fe I 6707.441Å line contribution, determined by an empirical (B-V) colour fit (see Soderblom et al. 1993b).
g− Li I 6708Å minus the Fe I 6707.441Å contribution.
h− Lithium equivalent widths are transformed into abundance [N(Li)] - on a scale where log N(H)=12, using a curve of growth in Soderblom et al. (1993b).

Internal[a] Identifier	JP96[b]	(B-V)$_o^a$	Temp[c] [K]	HJD[d] [(+2450000)]	RV [km s^{-1}]	Li I + Fe I [e] EW [mÅ]	Fe I [f] EW [mÅ]	Li I 6708Å[g] EW [mÅ]	N(Li)[h]
F3_0172	JP 49	0.811	5139	5223.713	-8.4	115	13	102	2.003
F3_0215	JP 41	0.874	4946	5223.712	-7.4	153	14	139	1.985
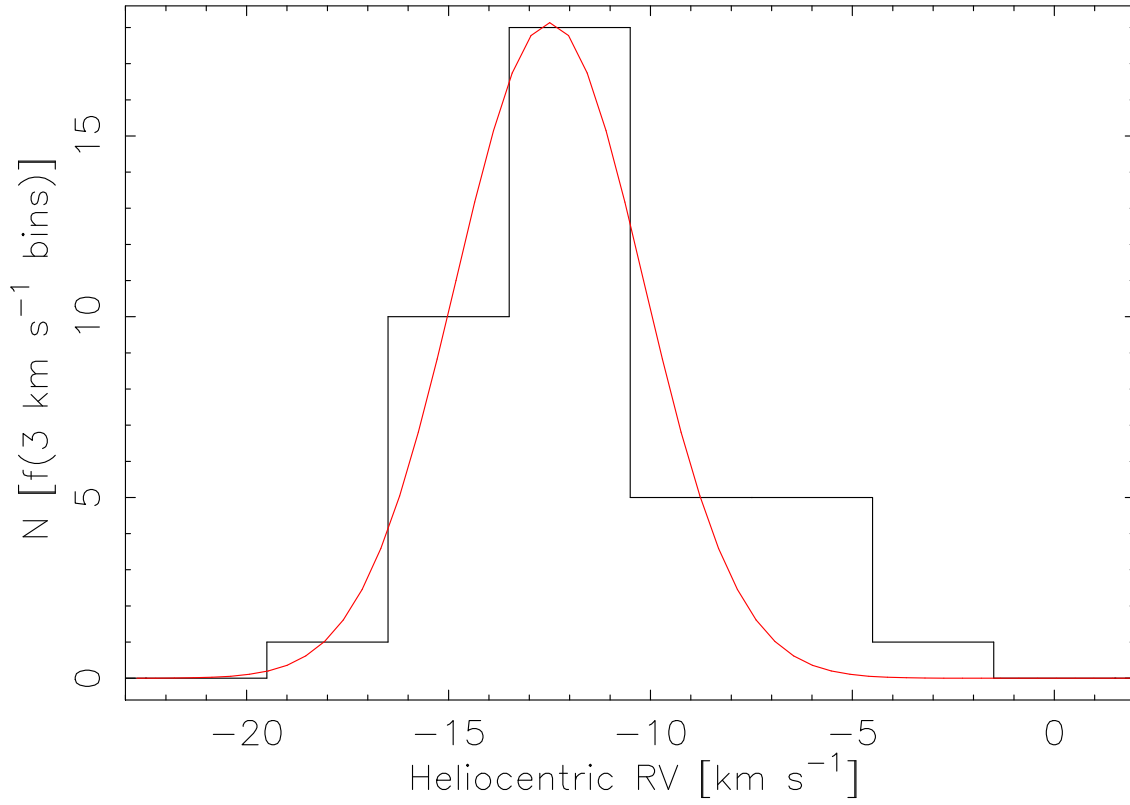
Fig. A.1. Heliocentric radial velocities, in histogram form using 3 km s^{-1} bins, are plotted for M 34 stars using velocity data detailed in Jones et al. (1997). The red solid line depicts an unweighted Gaussian fit to the data, with a Gaussian centre of -12.49 km s^{-1} and a sigma of 2.32 km s^{-1}.
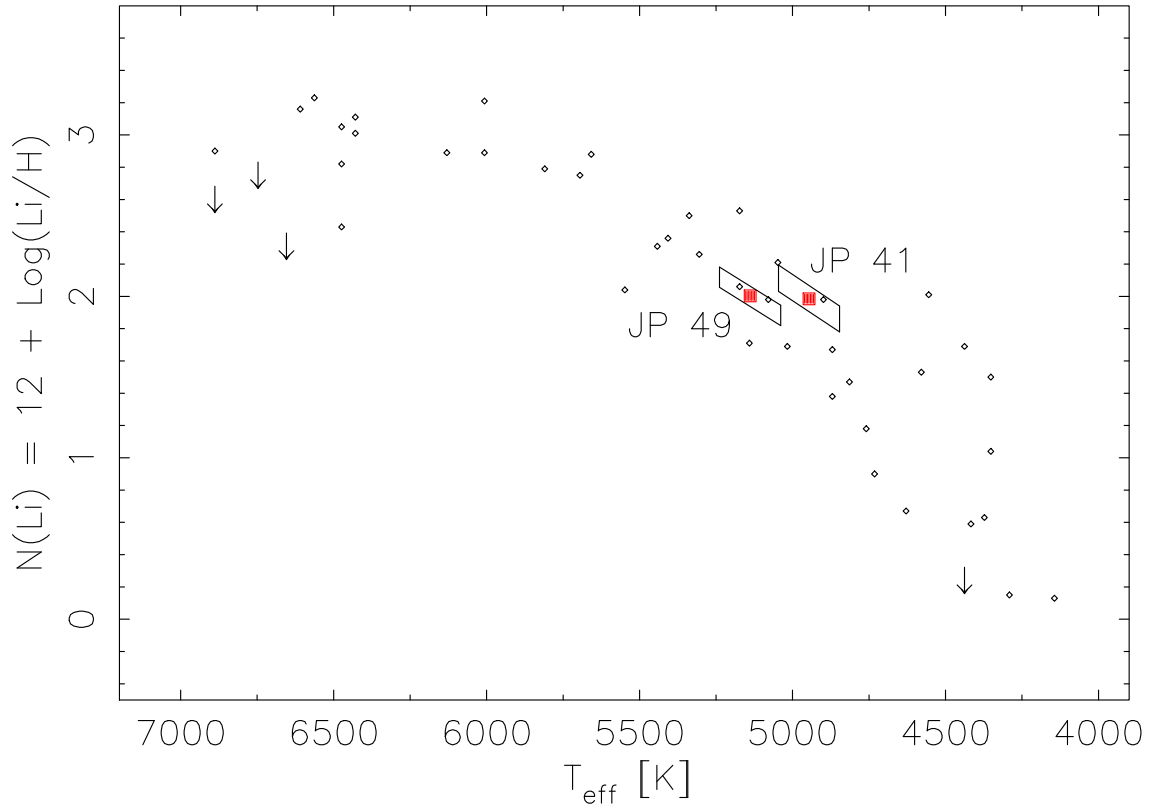
Fig. A.2. Logarithmic lithium abundances N(Li) = 12 + log(Li/H) versus effective temperature are plotted for stars in the M 34 cluster (data taken from Jones et al. 1997). Red filled squares represent abundances for F3_0172 & F3_0215 (JP 49 & JP 41), determined using data reported in Table A.2, with error parallelograms based on temperature errors of 100 K and 15% equivalent width uncertainties.

Appendix B: A Period vs Equatorial Velocity Analysis

A comparison of photometric period and projected equatorial rotation rate for M 34 stars is plotted in Fig., B.1. For the most part, photometric periods are determined from the Lowell campaign described in this manuscript, except for a few cases where Irwin et al. periods are employed where Lowell ones do not exist. Spectroscopic velocities for stars in common to the Lowell campaign and Irwin et al. survey are obtained from Jones et al. (1997). Three loci are also shown in the figure, representing equality between period and $v \sin i$ data for G0, K0 & M0 dwarfs, where $\sin i = \pi/4$ is assumed for each.

There are three notable characteristics to the plot. First, the clustering of data-points for stars with periods $\simeq 6.5 \rightarrow 9$ days and $v \sin i \simeq 10 - 14$ km s^{-1} lie to the right of the G0 dwarf locus. Given that the M 34 stars having photometric periods are late-F to early M-dwarfs, these data-points are most likely indicative of those stars whose $\sin i$ values are $> \pi/4$. Second, there are four stars with periods < 3 days and $10 < v \sin i < 25$ km s^{-1}, whose period, $v \sin i$ data place them considerably below even the M0 dwarf locus in the diagram. Assuming that these stars are *bona fide* cluster members, whose period and $v \sin i$ values are correctly determined, these stars must be high inclination systems ($\sin i < \pi/4$; *i.e.,* becoming more pole-on), whose true equatorial velocities are considerably higher.

Finally, there is one M 34 star (F3_0258) whose period determinations, from our Lowell data and by the Irwin et al. study, are seriously discrepant (see also Fig., 2). The periodicity for this star was detected in three filter/exposure time observations during our Lowell campaign. It is interesting to note that the Irwin et al. period is almost half that of our Lowell one, and their lower value could be due to phase aliasing, power leakage in the power spectrum as a consequence of their shorter observing window or multiple spot groups on the surface on the star during its observation. In any case, either both period determinations are incorrect, or either value from the Lowell campaign or the Irwin et al. study is in error.

If we assume that one of the periods for this star is correct, we can make some predictive statements as to its equatorial velocity. With an intrinsic B-V colour of 0.95, its spectral type on the main sequence would be K2 or K3, placing it close to the central locus of the three plotted in Fig., B.1 (assuming the star is inclined 45° to the line-of-sight). This scenario is consistent with its Irwin et al. period of 6.655 days. Conversely, if the Lowell period of 11.0 days is correct for this object, and it is a single member of the cluster lying on the main sequence, its inclination angle must be higher than 45° ($\sin i > \pi/4$), whose appearance is more face-on to the line-of-sight. Hopefully, more extensive photometric monitoring of this star will reveal its true nature.
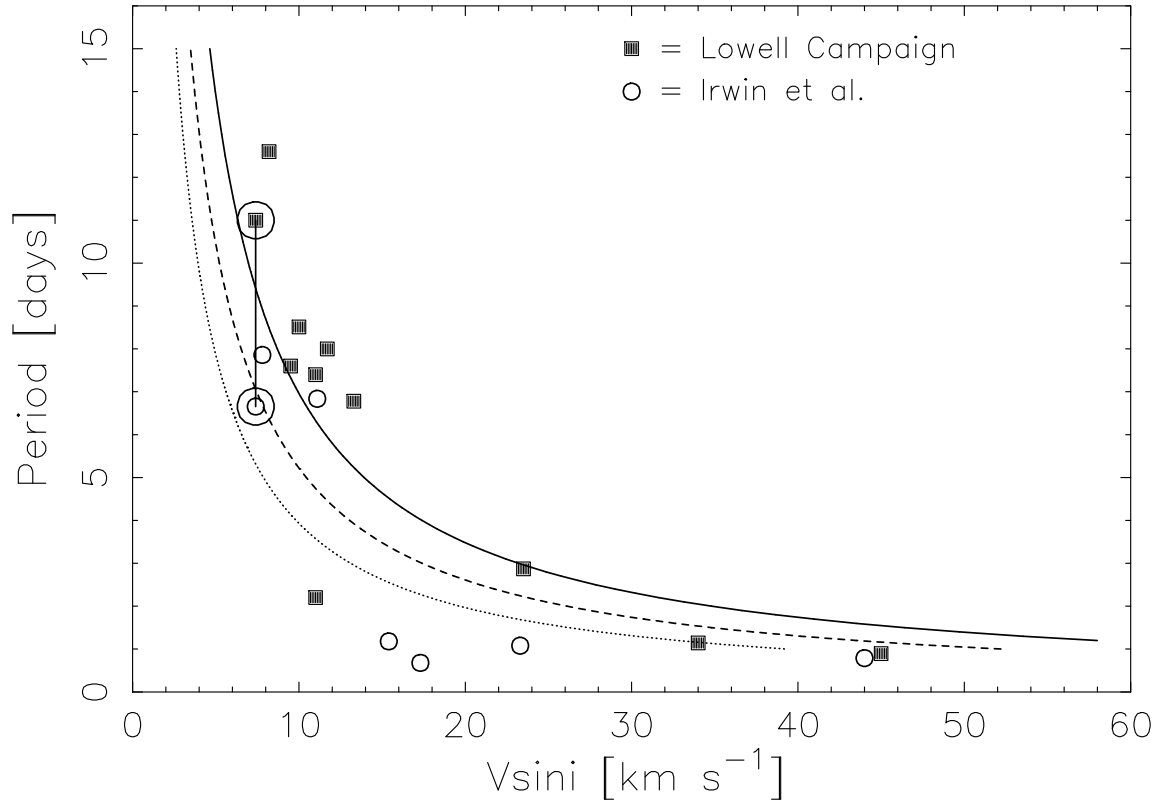
Fig. B.1. Projected equatorial velocities (*v* sin *i*) are plotted for those M 34 stars having corresponding photometric periods derived during the course of the Lowell campaign. *V* sin *i* data are taken from Jones et al. (1997). For those cases where there is no Lowell campaign period available, similar data from the Irwin et al. (2006) sample are presented. One exception is shown for the star F3_0258, linked by a straight solid line, whose Lowell campaign and Irwin et al. periods are seriously discrepant (11.0 ± 1.0 and 6.655 days respectively). Three loci are depicted representing equal period-vs-*v* sin *i* relationships (assuming sin*i* = π/4) for G0, K0 and M0 dwarfs (solid, dashed and dotted lines respectively). In order of descending mass, stellar radii of R/R☉ = 1.08, 0.81 & 0.61 were employed (Gray 1992).

Appendix C: Lowell Light-curves for
Photometrically Variable Stars in the Field of
M 34
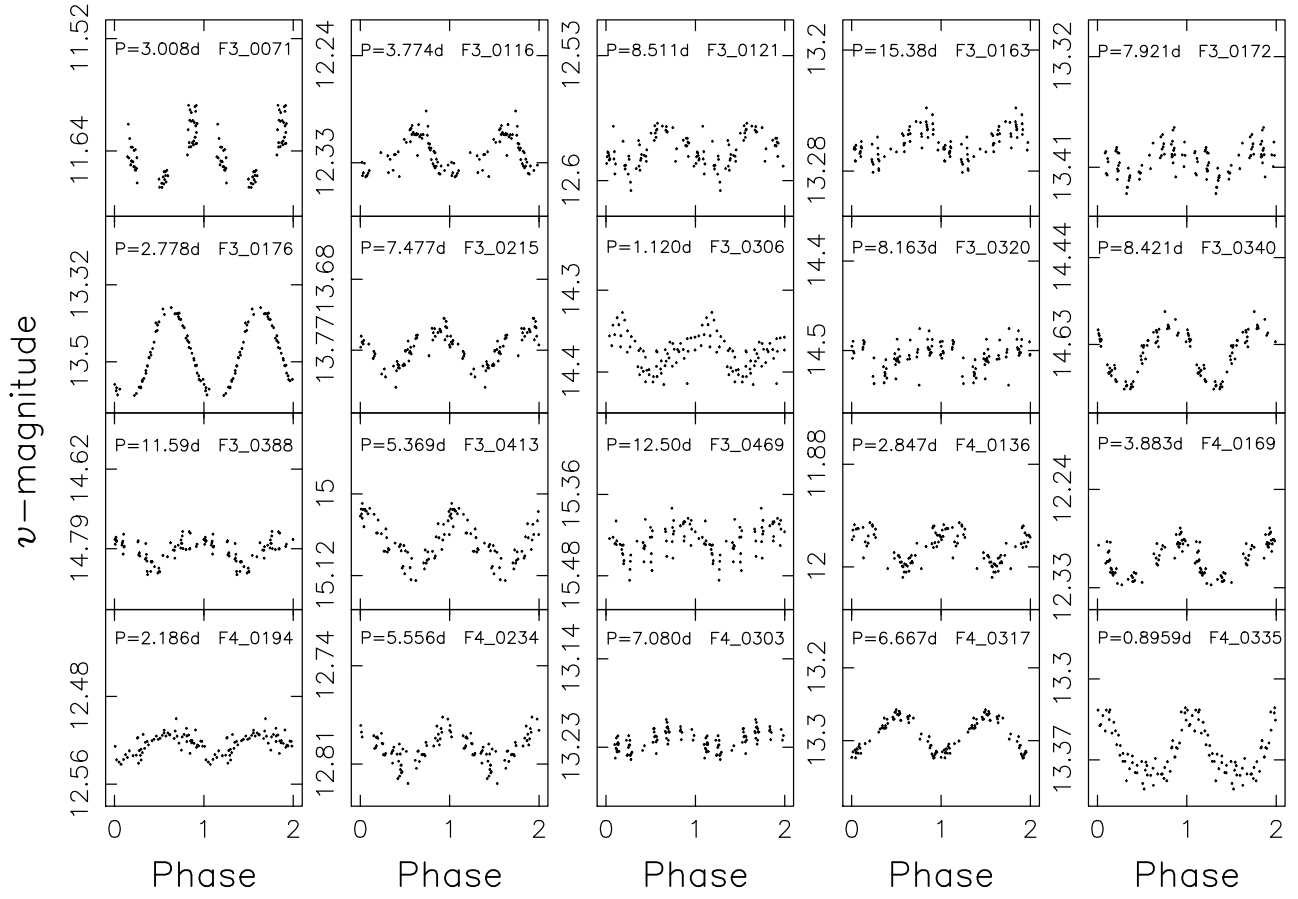
Fig. C.1. Period-phased photometric lightcurves for M 34 variables, derived from short-V observations.
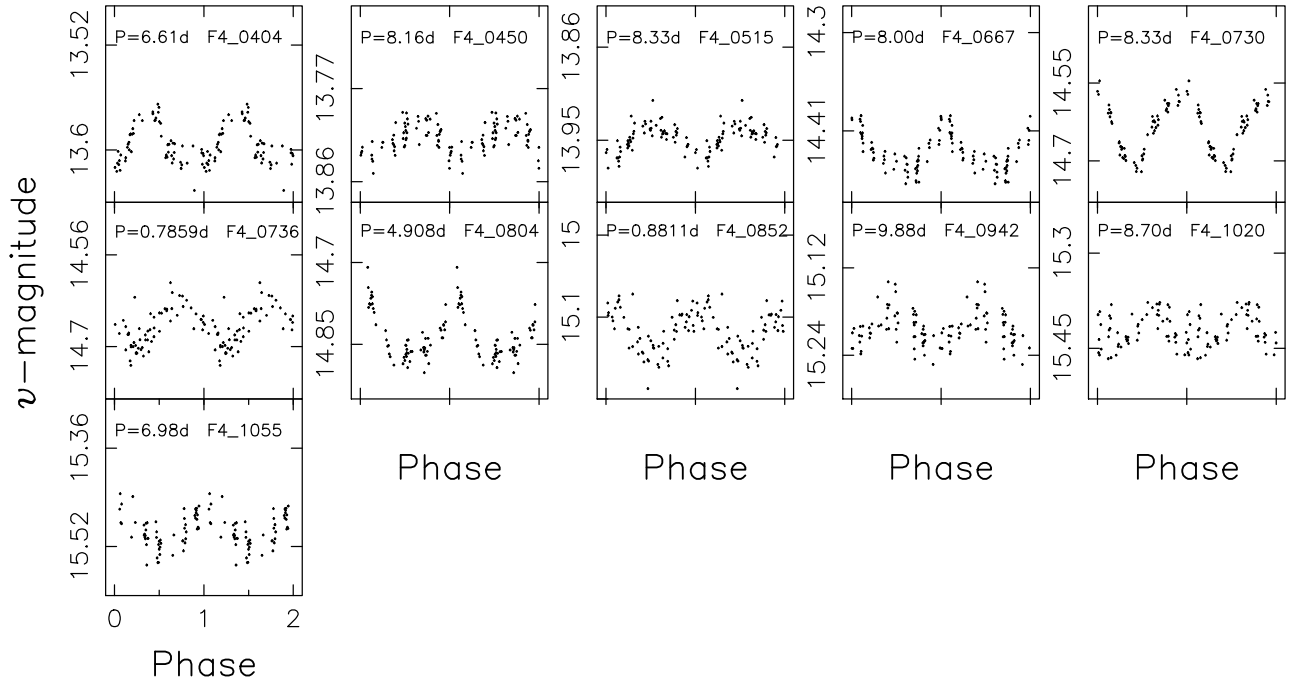
Fig. C.1 Cont/d....
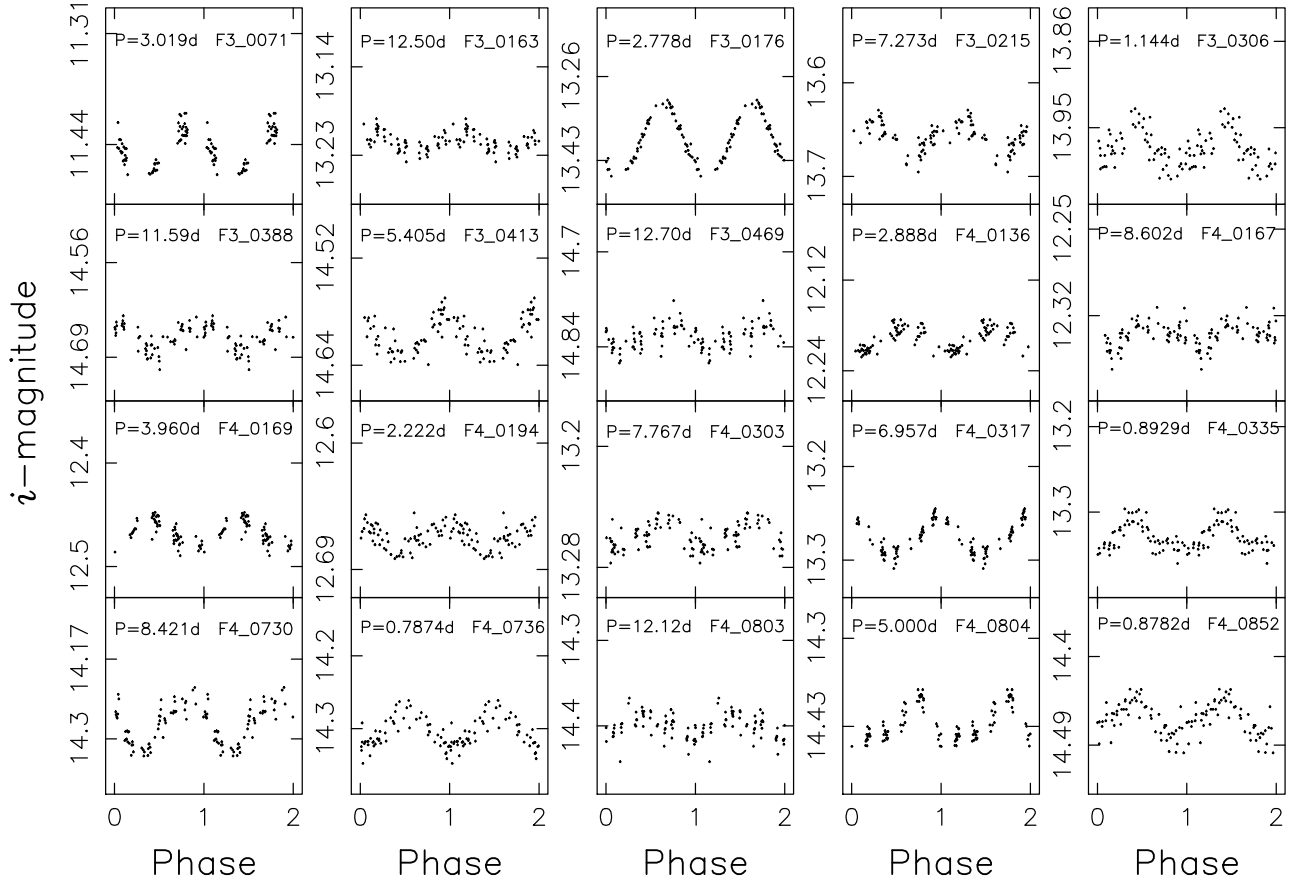
Fig. C.2. Period-phased photometric lightcurves for M 34 variables, derived from short-I observations.
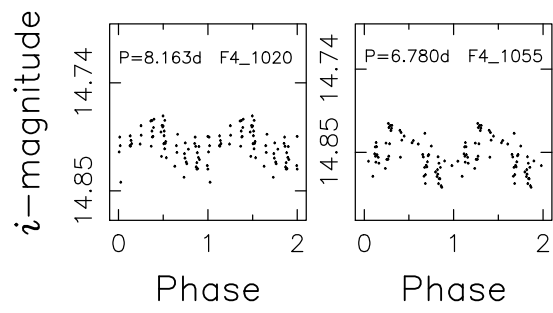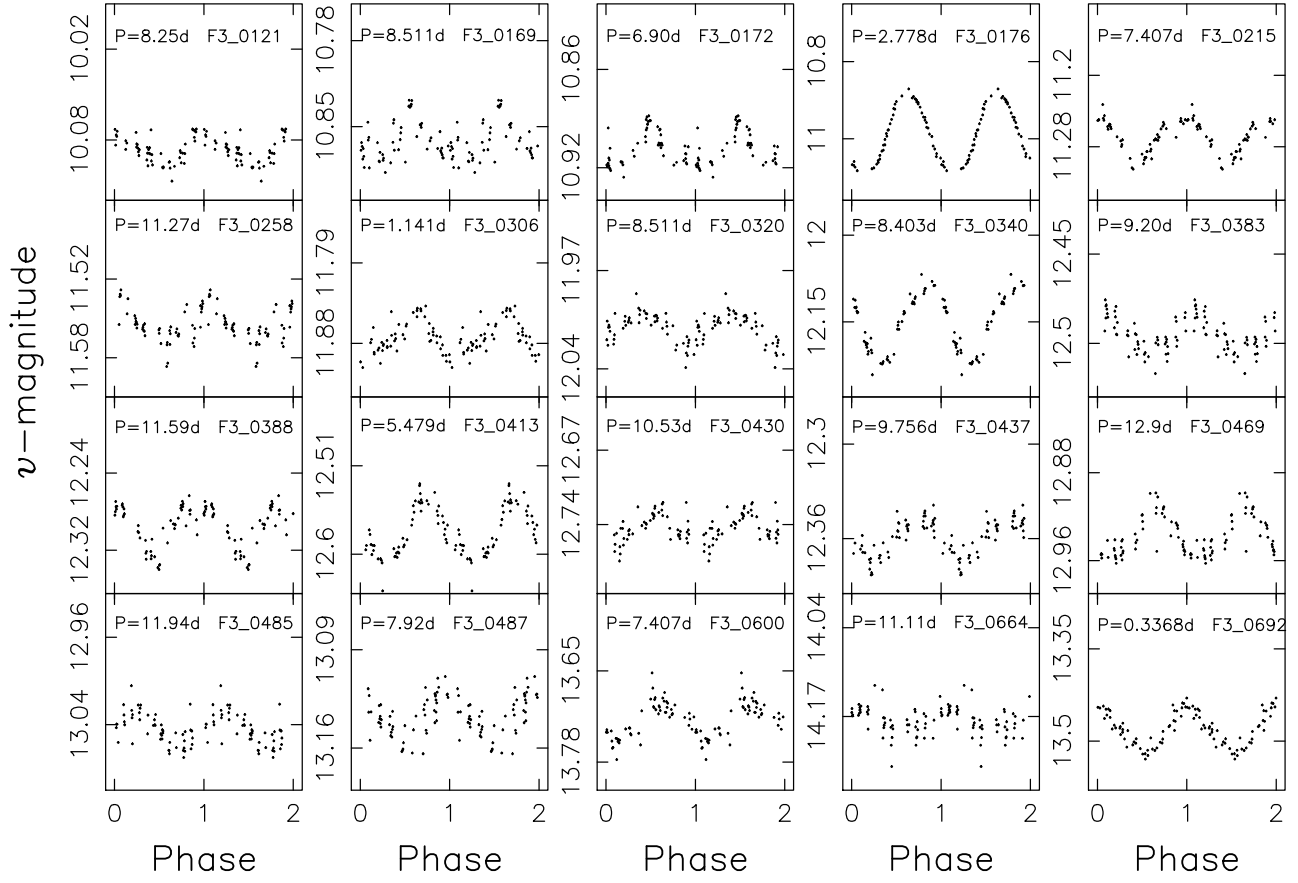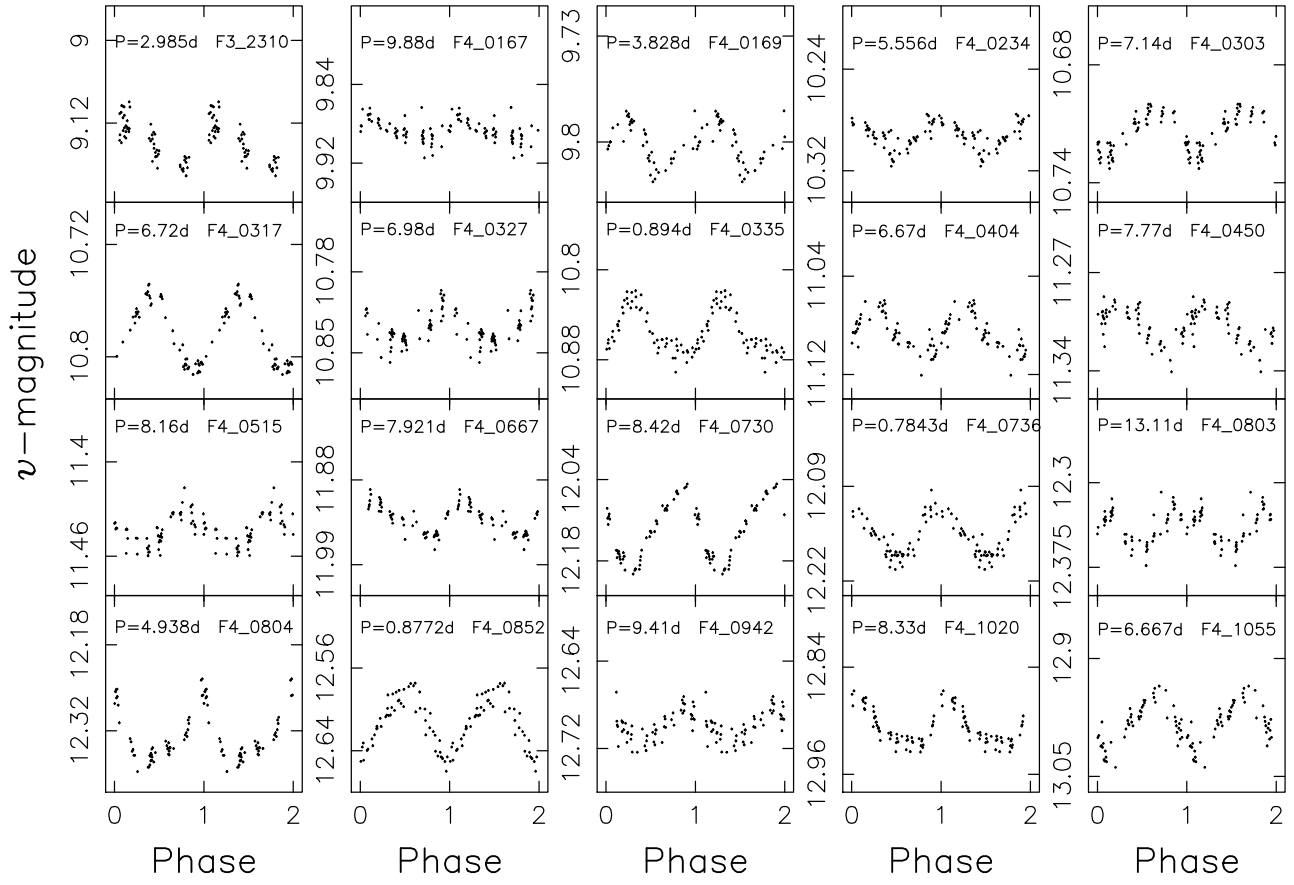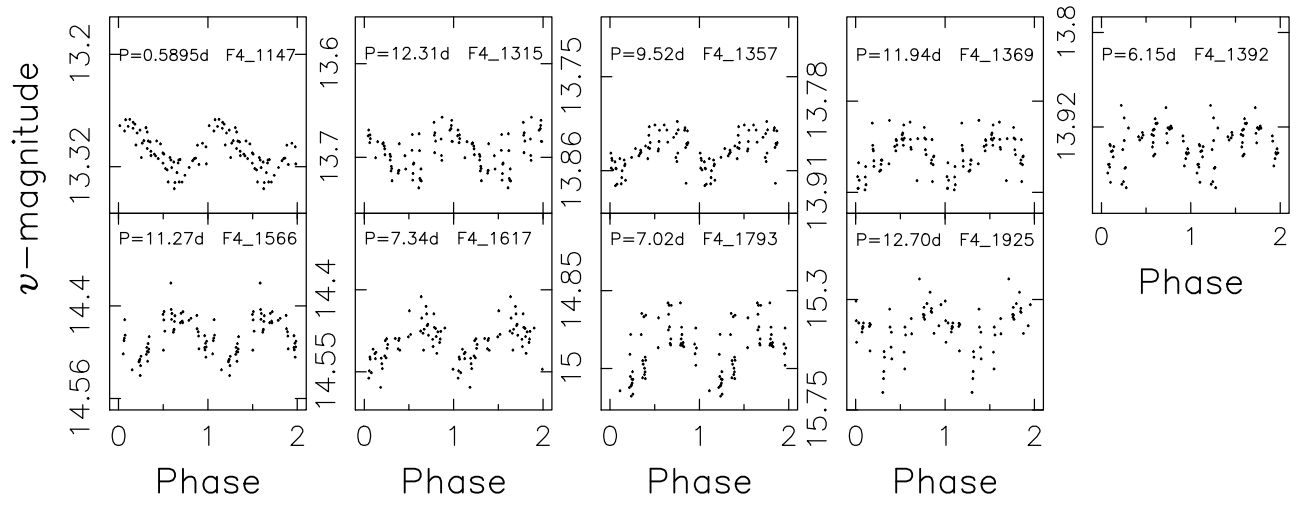
Fig. C.2 Cont/d....

Fig. C.3. Period-phased photometric lightcurves for M 34 variables, derived from long-V observations.

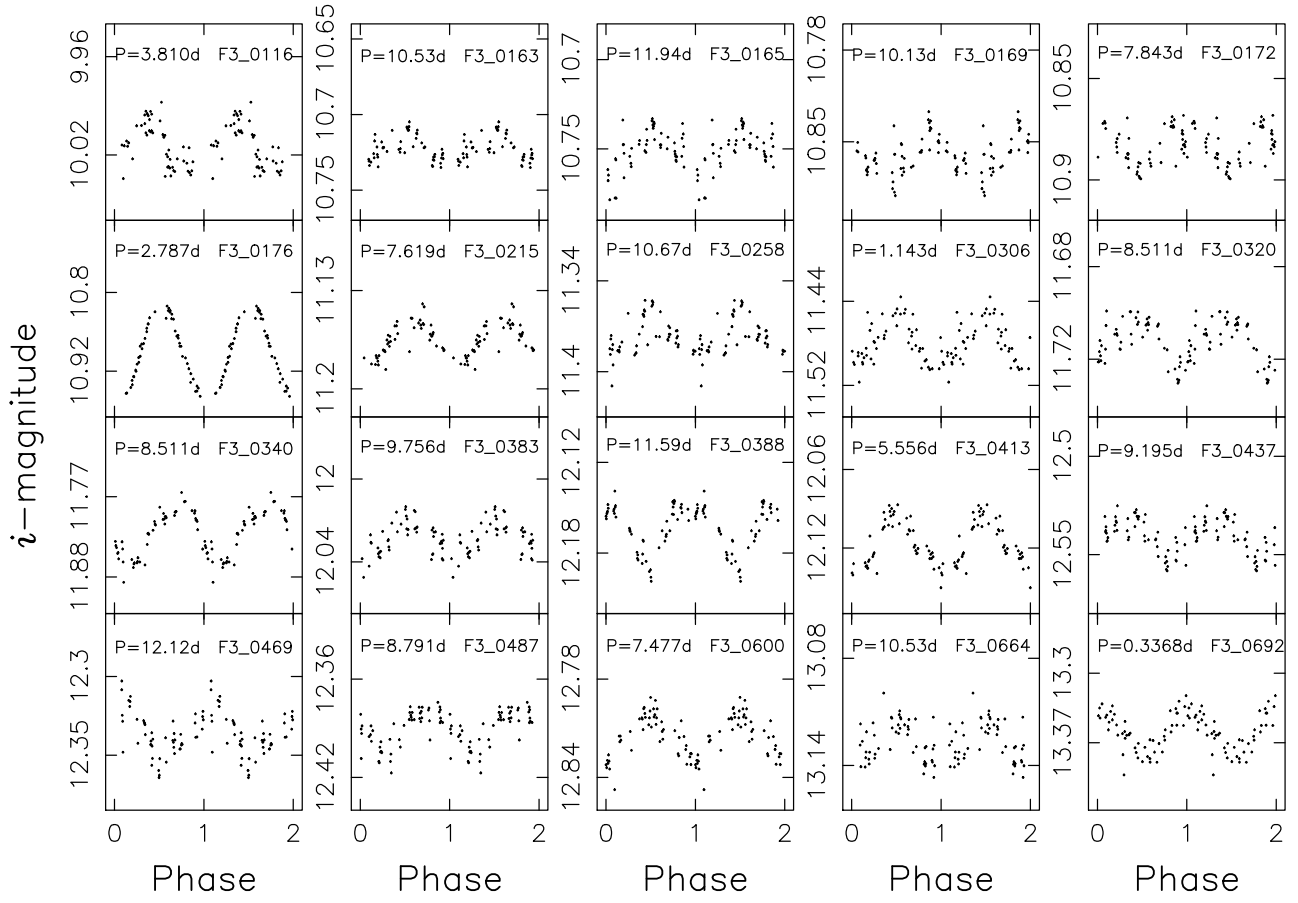**Fig. C.3** Cont/d....

Fig. C.3 Cont/d....

Fig. C.4. Period-phased photometric lightcurves for M 34 variables, derived from long-I observations.
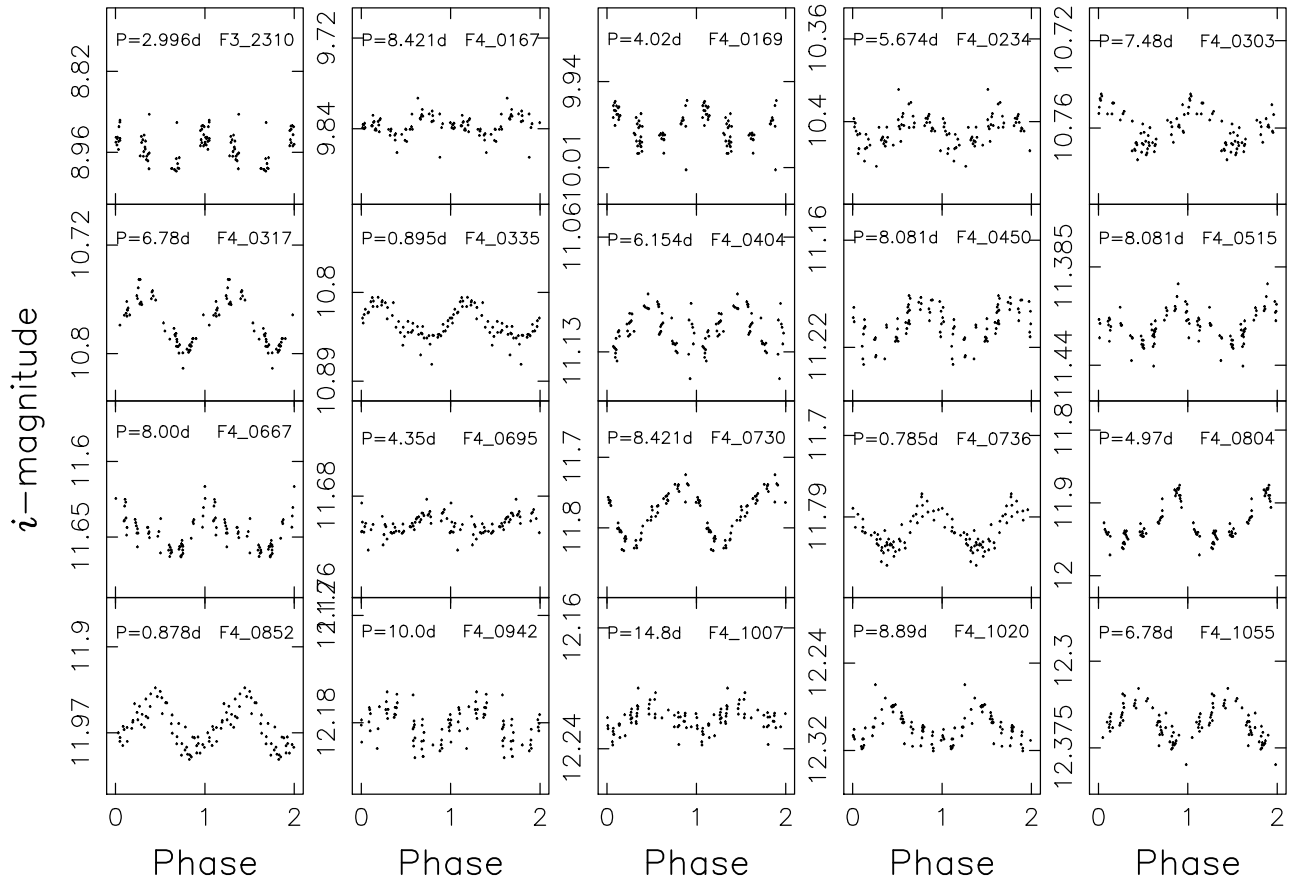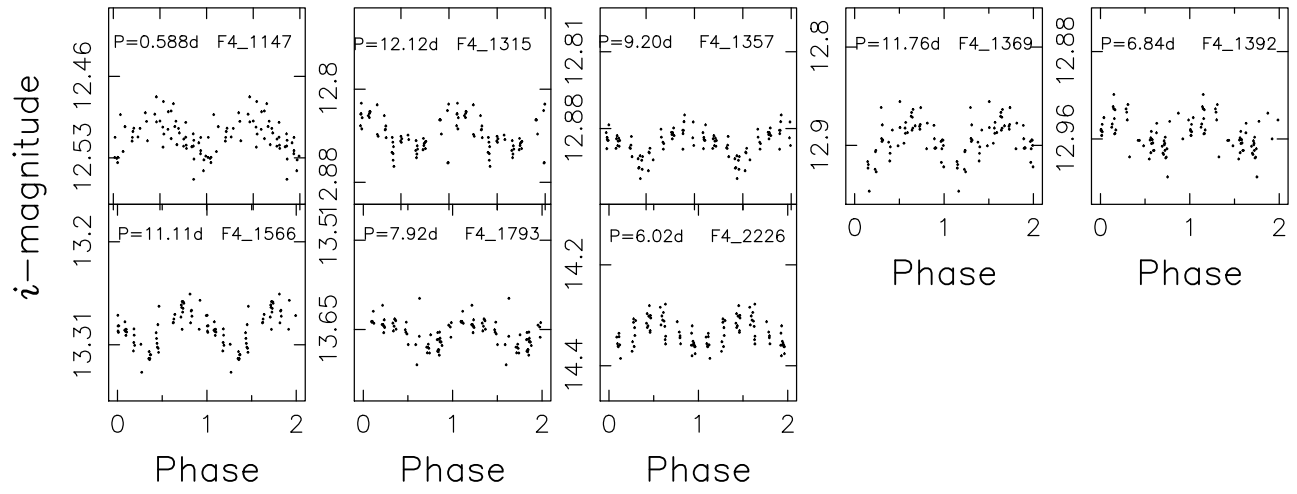
Fig. C.4 Cont/d....

Fig. C.4 Cont/d....